LBNL-40486
UC-1501

ERNEST ORLANDO LAWRENCE BERKELEY NATIONAL LABORATORY

The Science of Electrocatalysis on Bimetallic Surfaces

Philip N. Ross Jr.

Materials Sciences Division

June 1997

An excerpt in
Frontiers in Electrochemistry
J. Lipkowski and
P.N. Ross Jr.,
Vol. 4,
Wiley-Interscience,
New York, NY, 1997

REFERENCE COPY
Does Not
Circulate
Bldg. 50 Library - Ref.
Lawrence Berkeley National Laboratory
Copy 1
LBNL-40486

DISCLAIMER

This document was prepared as an account of work sponsored by the United States Government. While this document is believed to contain correct information, neither the United States Government nor any agency thereof, nor the Regents of the University of California, nor any of their employees, makes any warranty, express or implied, or assumes any legal responsibility for the accuracy, completeness, or usefulness of any information, apparatus, product, or process disclosed, or represents that its use would not infringe privately owned rights. Reference herein to any specific commercial product, process, or service by its trade name, trademark, manufacturer, or otherwise, does not necessarily constitute or imply its endorsement, recommendation, or favoring by the United States Government or any agency thereof, or the Regents of the University of California. The views and opinions of authors expressed herein do not necessarily state or reflect those of the United States Government or any agency thereof or the Regents of the University of California.

LBNL-40486

THE SCIENCE OF ELECTROCATALYSIS ON BIMETALLIC SURFACES

Philip N. Ross Jr.

Materials Sciences Division
Lawrence Berkeley National Laboratory
University of California
Berkeley, CA 94720

Acknowledgment

The author is pleased to acknowledge the continuing financial support for our research in electrocatalysis from the Assistant Secretary for Energy Efficiency and Renewable Energy, Office of Transportation Technologies, of the U.S. Department of Energy under contract No. DE-AC03-76SF00098.

THE SCIENCE OF ELECTROCATALYSIS ON BIMETALLIC SURFACES

Philip N. Ross, Jr.

Materials Sciences Division

Lawrence Berkeley National Laboratory

Berkeley, California 94720

INTRODUCTION

In this chapter I will review progress in the fundamental science of electrocatalysis on metallic surfaces. The focus will be on two types of metallic surfaces: single crystal surfaces of pure metals, and bimetallic surfaces. Two types of bimetallic surfaces will be discussed, the surfaces of bulk alloys, and pure metal surfaces modified by the deposition (usually by underpotential deposition or UPD) of a second metal. The preponderance of electrocatalytic reactions studied on these surfaces are those related to the development of low temperature fuel cell technology, *e.g.* oxygen reduction and methanol oxidation. The chapter in this same Volume by Adzic covers studies of oxygen reduction on single crystal surfaces of pure metals, and thus the presentation here will cover oxygen reduction on bimetallic surfaces and on the oxidation of methanol and other C_1 compounds on both pure metal and bimetallic surfaces. As in previous Volumes in this series, the emphasis is on advances in the fundamental science, and no attempt is made to

provide a comprehensive review of developments in "real", *i.e.* high surface area, electrocatalysts. A brief overview of new electrocatalysts is, however, presented in cases where these materials have motivated new fundamental studies.

BIMETALLIC SURFACE CHEMISTRY

Bimetallic electrodes can be prepared in a number of ways, some methods being unique to electrocatalysis. In addition to all the ways one can prepare a bimetallic surface for studying non-electrochemical reactions, one can also use a variety of electrodeposition techniques to prepare a bimetallic surface *in-situ*. Electrodeposition methods have the advantage of not requiring any additional equipment for the preparation of the surface other than the galvanostat/potentiostat being used to measure the reactivity. It is also a fast method of preparation and is particularly advantageous method for screening the reactivity of candidate bimetallic catalysts. For fundamental studies of reactions on bimetallic surfaces, as, for example, studies aimed at determining how the pathway changes on a pure metal surface with the introduction of a second metal to the surface, the electrodeposition method of preparation has the major drawback of creating an unknown surface, or a much more complicated problem of characterizing the surface than if one prepares the surface ex-situ. Therefore, the emphasis in this chapter will be on the preparation and characterization of metallic and bimetallic surfaces ex-situ, with subsequent transfer of the well-characterized surface into an electrochemical cell for analysis of reactivity. This approach utilities the full range of modern methods of both

bulk and surface characterization which is essential for developing a molecular level understanding of the reactivity of the surface.

Bulk Alloys

The most straightforward, but perhaps the most tedious, method of preparing bimetallic electrodes for fundamental studies is to prepare a bulk alloy by conventional metallurgy, *i.e.* melting the elements into an ingot followed by homogenization. This was the methodology employed in the seminal study of the direct oxidation of methanol by Pt alloys by Binder et.al. more than two decades ago [1]. That study was done before modern UHV tools of surface analysis were available, and so the major deficiency (only by today's standards) in that study was in the preparation of the surface and in the absence of a determination of the surface composition. With modern UHV methods of surface analysis, it is relatively easy to prepare the surface of a homogeneous bulk alloy in UHV accompanied by analysis of the surface composition by one or more analytical tools. This is the methodology which we have used in my laboratory to re-examine the direct oxidation of methanol on a number of Pt alloys included in the study by Binder et.al. As described later in this chapter, our re-examination of Pt-Ru, for example, found a heretofore unknown sensitivity of the reactivity to the surface composition of this alloy, illustrating that there is still much to be learned about alloy electrocatalysts, even those that have been studied frequently in the past.

The difference between the surface and the bulk composition of alloys has been the subject of intensive research, in both theory and experiment, in the last two decades, and a review of the subject is beyond the scope of this chapter. Excellent reviews of both

theory and experiment have been presented by Campbell [2] and by Dowben and Miller [3], and earlier by Sachtler and Van Santen [4] and Chelikowski [5]. The encyclopedia of surface structures by Watson et. al. [6] is also an excellent place to find references to a specific alloy or metal-on-metal system. It is now widely recognized that surface segregation, *i.e.* the enrichment of one element at the surface relative to the bulk, is a ubiquitous phenomenon in bimetallic alloys, and the theory for accounting for and predicting this segregation is well-developed. Yet surface segregation has been an entirely neglected phenomenon in a disturbingly large number of papers in alloy or other bimetal electrocatalysis. Therefore, it seems appropriate to provide here a brief review of both the basic principles of surface segregation and the current state of experiment, with a focus on Pt alloys.

The most reliable method for determining the composition of the outermost layer of atoms of a polycrystalline bulk alloy is by low energy ion scattering (LEIS) using inert gas ions like helium and neon. An excellent review of the physics of LEIS is provided by Heiland and Taglauer [7]. A brief overview is provided here. A schematic representation of the primary phenomena in LEIS is shown in Figure 1. The extreme surface sensitivity of this method lies in the large cross-section for neutralization of rare gas ions by metals, *e.g.* the ratio of ions scattering from the first layer to those from any layer below is about 10^5. A small fraction of the ions are scattered elastically from the surface atoms with an energy loss that is described by a binary single-scattering model. The energy loss is related to the mass of the surface atom and the mass of the ion by the relation given in the Figure. Energy analysis of the scattered ions can be done with a

variety of spectrometers, including most modern electron spectrometers used in the same UHV system for x-ray photoelectron spectroscopy (XPS). Mass resolution is maximized and multiple-scattering can be minimized by using the backscattering geometry, $\Theta > 90^o$. Mass resolution, $M_s/\Delta M_s$, increases with increasing mass of the incident ion, and in principle it should be possible to separate the mass peak for ir from that of Pt with argon ions. But use of ions heavier than Ne has a number of problems: the cross-section for back-scattering is reduced, and with increased forward scattering multiple-scattering is much more significant; the result is reduced signal intensity and a multiple-scattering tail that makes mass resolution more difficult; there is also the undesirable side effect of significant sputtering of the surface during the analysis. In our experience with Pt-rich alloys, it is quite difficult to resolve the scattering peak for any element with $\Delta M < +/-10$, *i.e.* from Re to Pb. Quantitation of LEIS spectra from alloys is best obtained by measuring elemental sensitivity factors from the pure metals in the same apparatus under identical conditions. Matrix effects are generally not important in LEIS, so the straightforward use of elemental sensitivity factors appears to result in very accurate quantitation [8].

An example from my laboratory of an LEIS spectrum from a Pt-Ru alloy electrocatalyst is shown in Figure 2. Details of the analysis are given in Gasteiger et. al. [9]. The bulk alloy composition is 70.2 % Pt, but the annealed surface, which is the spectrum shown, has a composition of 92.1 % Pt. The Ru peak, with a ΔM of nearly 100, is easily resolved with He^+ ions even at the low surface concentration of ca. 8 %. The bulk concentrations can be produced on the surface as well by sputtering off the Pt-

enriched layer(s) with argon ions, for example. The Pt-Ru system is a classic example, as discussed in greater detail below, of surface segregation of the element having the lower heat of sublimation. The equilibrium surface composition of the Pt-Ru system as determined by LEIS by Gasteiger et. al. is shown in Figure 3. A compilation of other surfaces analyzed by LEIS has been made by Watson [10].

When the bulk alloy is prepared as a single crystal, one can use the powerful method of LEED (low energy electron diffraction) crystallography. This method is more specialized than LEIS, in that it requires a relatively sophisticated theory to interpret the LEED intensity data, and is best done in collaboration with practitioners of the method. As the name implies, with this method one gets not only surface composition information but detail about the atomic positions not only of atoms in the surface but in the sub-surface layers as well. One of the best illustrations of the power of LEED crystallography in alloy surface chemistry is the work by Gautier et. al. [11] on the surface and near-surface structure of $Pt_{50}Ni_{50}$ and $Pt_{78}Ni_{22}$. These alloys are very interesting from a theoretical perspective because the two metals have essentially identical surface energies, yet strong enrichment of the surface in Pt was observed by LEIS [12]. By LEED crystallography, Gautier et. al. found that the near surface region exhibits a highly structured compositional oscillation in the first three atomic layers of the (111) crystal, as shown in Figure 4. Such composition oscillations were previously thought to occur only in highly exothermic alloys, *i.e.*alloys with a high enthalpy of mixing, which are usually ordered in the bulk as well, Pt_3Sn being the prime example [4]. The Pt-Ni alloys are disordered in the bulk and have only small enthalpies of mixing. The so-called size

effect, *i.e.* the tendency for the larger atom to be at the surface [13], must be treated rigorously to account for the compositional oscillation in this system, as done by Treglia and Legrand [14].

For polycrystalline alloys, composition profiles below the surface can be obtained by the judicious use of LEIS combined with either Auger electron spectroscopy (AES) or XPS. Since one has to model the electron emission from atoms below the surface to interpret the data, the reliability of these determinations is improved if AES or XPS spectra are acquired with an angle-resolving electron spectrometer at various take-off angles (angles of emission with respect to the surface normal). Composition profiles below the surface are of interest primarily for purposes of testing theories of segregation. However, in cases where there is extreme enrichment, as, for example, when the first layer is composed entirely of one constituent, it is important to know the composition of the second layer to evaluate possible electronic effects in the catalytic properties of the alloy. In the case of $Pt_{78}Ni_{22}(111)$, for example, the catalytic properties of the pure Pt surface of this alloy is possibly different from the properties of Pt(111) due to the intermetallic bonding with Ni in the second layer. In fact, alloys with this type of enrichment provide a useful test of the so-called electronic factor in alloy electrocatalysis, as we discuss in a later section.

The state of the theory of surface segregation in bulk alloys is now quite advanced and there are now several theories that should be considered highly reliable predictors of the equilibrium surface composition. The body of work on the theory of segregation is too large to review in the context of this chapter. It is, however, useful in the context of

later sections to provide a brief overview of the state of theory. An excellent review of early work on what I would call chemical models of segregation is provided by Kelley and Ponec [15]. More recently, King [16] has provided an update on the state of chemical models and Mazurowski and Dowben [17] have provided a compilation of experimental results and a comparison with the prediction of three different theories. By far the most successful of the three theories is that of Mukherjee and Moran-Lopez [18], which is an electronic model. Chemical models are of two types: a macroscopic thermodynamic approach that incorporates knowledge of the surface tension of the pure components, the enthalpy and entropy of mixing, and the molar surface areas in a classical Gibbsian thermodynamic framework; and a so-called bond breaking or broken bond models, which use a detailed knowledge of bond energies and nearest-neighbor coordination in the surface region to minimize the total energy. The basic tenet of chemical models is that the component with the lowest heat of sublimation will segregate to the surface. Chemical models have two fundamental limitations: a.) the necessary chemical properties of the pure constituents and/or the mixing properties (or bond energies) may not be known or be very accurate; b.) the strain energy introduced when there is a large difference in atomic radii is not treated adequately. Chemical models fail to predict the correct enrichment in systems where the constituents have comparable sublimation energies but significant differences in atomic radii, *e.g.* the Pt-Ni system.

Electronic models, in essence, calculate all of the needed chemical properties from the electronic properties of the pure constituents and the alloy in a way which may not be exact for any one system but is consistent. Mukherjee and Moran-Lopez, for example,

employ a tight-binding electronic theory which uses a simple form of the d-band density of states (DOS) of the pure components with bandwidth, band center and band filling as the only input parameters. Interestingly, Treglia and Legrand used a tight-binding framework to calculate the strain energy in the Pt-Ni system, and produced quantitative agreement with the composition profiles from LEED crystallography. Another more sophisticated electronic model is the use of Monte Carlo simulation techniques with the energetics described by the Embedded Atom Method (EAM), as described in the review by Foiles in a recent review article [19]. The EAM calculation allows the relative atomic positions to adjust to the compositions so that lattice strain energies and even vibrational contributions are incorporated. The EAM calculations have so far been applied to a smaller but important subset of transition metals than the other theories, the binary alloys of the fcc metals, Cu, Ag, Au, Ni, Pd and Pt. Foiles et. al. [20] have reported the segregation energies for the first two atomic layers for the 25 combinations of metals in this group, which can be used to calculate the compositions of these layers for any bulk composition. A rather surprising result of these calculations is that the composition profile is predicted to oscillate in many of these alloys, contrary to the predictions of chemical models for these same alloys. These oscillations appear to be due to strain energies due to the size mismatch (> 10 %) in many of these combinations.

Because of the importance of Pt alloys in electrocatalysis, the predictions from current theories of surface segregation for a wide variety of Pt alloys are shown in Figure 5. Although there has not been experimental confirmation of all these predictions, I know of no convincing experimental contradictions to these predictions. An interesting and

perhaps unrecognized (by electrochemists) feature of the results in this figure is that enrichment of the surface in Pt is the rule rather than the exception ! In fact, for Pt-rich bulk compositions, *e.g.* Pt_3M, there are a significant number of alloys for which the annealed surface is pure Pt, including the isoelectronic series Ti, Hf, and Ta, and the 3 d metals Fe, Co and Ni. Surface enrichment in Pt alloys is, therefore, ubiquitous and an extremely important phenomenon in electrocatalysis both from a fundamental and technological viewpoint. That is, of course, the principal reason why this phenomenon receives relatively detailed discussion in this chapter. The consequences of this segregation on the electrocatalytic properties of Pt alloy surfaces are clearly evident in well-designed experiments, as we shall see in a later section.

Pt_3Sn occupies a special place in both alloy surface chemistry and in alloy electrocatalysis. It is a highly exothermic alloy, with an enthalpy of formation of - 50.2 kJ/g-atom [21], that crystallizes in the Ll_2 (Cu_3Au-type) lattice, as shown in Figure 6. This alloy played an important role in the development of the broken-bond model for segregation in highly exothermic, ordered alloys [4] and polycrystalline samples were the subject of intense experimental examination by Van Santen and co-workers [21] using a variety of methods, including LEIS. These results with polycrystalline samples appeared to validate the broken-bond model, since the observed surface composition of ca. 50 % Sn is in agreement with the model prediction. In my laboratory, in collaboration with Ugo Bardi both in Berkeley and later in Florence, we conducted the first studies of segregation with single crystals of Pt_3Sn, using both LEIS and LEED crystallography. These studies are described in a series of papers [22] and a review of the work has already

been presented by Bardi [23]. The single crystal results revealed that the broken-bond model does not, in fact, get the details of the segregation quite right. The model correctly predicted an absence of segregation on the (111) surface, but incorrectly predicts that the pure-Pt (200) planes are enriched in Sn by exchange of atoms with the second atomic layer. This does not occur, rather the crystal is terminated preferentially in the compositionally mixed (100) plane by the formation of double-height steps. A similar preferential termination in the compositionally mixed (220) plane occurs for the <110> orientation. Pt_3Sn is the most active catalyst known for the electrochemical oxidation of carbon monoxide (CO), and the different low index surfaces just described have remarkably different activity for this reaction, as discussed in detail in a later section.

There is another ordered Pt alloy that is isostructural with Pt_3Sn whose surface chemistry has been studied in some detail, Pt_3Ti. The first studies of Pt_3Ti single crystal surfaces were also performed in my laboratory in collaboration with Ugo Bardi. The first qualitative LEED and AES studies [24] appeared to show bulk termination surface structures in the compositionally mixed planes, but later studies by LEIS [25] reported that both the <100> and <111> orientations are terminated by pure Pt layers. More recent LEED crystallography studies [26] have confirmed the LEIS result, which among other things demonstrates the difficulty in determining the composition of the outermost atomic layer by AES (or XPS) when there is strong enrichment. While preferential termination of the <100> orientation in the pure Pt plane would not be surprising, (in fact, it is predicted by the broken bond model [27]) the pure Pt layer on the (111) surface is, particularly since the second layer and succeeding layers are bulk layers. This unusual

result could be due to a slight excess of Pt from the 3:1 stoichiometry (all published results on Pt_3Ti have come from samples cut from the same rod prepared in this laboratory); the accuracy in determining the bulk composition was only +/- 1 %. The broken bond model calculation for Pt_3Ti by Spencer [27] demonstrated an extreme sensitivity of Pt segregation to the (111) surface on the bulk stoichiometry, *e.g.* even to a Pt excess as small as 0.1 %. A slight excess of Pt can also be produced experimentally by extended ion bombardment due to preferential sputtering of Ti. Whatever the mechanism, it is clear that Pt_3Ti surfaces, after the usual UHV treatment of sputter-cleaning and annealing, are all pure Pt, and thus are in a similar category to Pt-Ni and Pt-Co (Pt-rich alloys). Thus, we have three different alloy systems which can be studied specifically for the elusive "electronic effect" in electrocatalysis, as discussed in a later section.

Overlayers and Surface Alloys

Another method for producing a bimetallic surface, besides the preparation of a bulk alloy of the two metals of interest, is to deposit one metal on the surface of another. The deposition may be by a variety of methods, including electrodeposition, and is often followed by thermal annealing. There is an enormous advantage for fundamental studies to doing this deposition in a UHV system equipped with the same tools of surface structure/composition analysis described above, LEIS and LEED. This method of producing bimetallic surfaces has been exploited to a much greater extent in gas-phase catalysis than in electrocatalysis, and, in fact, one of my purposes here is to provide a tutorial in the hope of promoting greater use of the method for electrochemical studies.

Reviews of the study of adsorption and catalysis on overlayer structures can be found in the report by Rodriguez and Goodman [28] and in the chapter by Campbell [2]. The review by Rodriguez and Goodman emphasizes the use of CO as a probe molecule for elucidating the elusive electronic effect in catalysis. Large shifts in the desorption energy for CO adsorbed to (nominal) saturation in UHV are reported for very thin films of Pd (1 to 2 ML) on Ta(110) and W(110), which appear to be correlated to strong intermetallic bonding and orbital mixing between the two metals. Unfortunately, there have not as yet been any studies of catalytic reactions involving CO, such as CO oxidation, conducted on these structures to see how these changes in bond energy effect the reactivity. On the other hand, Campbell in his chapter shows how submonolayers of an inert adatom, bismuth, can be used to study the ensemble effect in reactions involving the dehydrogenation of simple hydrocarbons on the Pt(111) surface. Free Pt surface atoms are needed in these reactions, because they extract the hydrogen atoms from the hydrocarbon. The reaction can be written in general terms as

$$C_xH + A[Pt] \Longrightarrow nH_{ads} + C_xH_{y-n} \qquad \{1\}$$

where A is the ensemble of free Pt atoms need for H extraction. What is surprising in these results is that the ensemble requirements are large: 5 - 10 for cyclopentene, 8 - 13 in cyclohexane, and 6 - 11 for benzene. These Pt ensemble requirements for dehydrogenation steps are very relevant to hydrocarbon oxidation on Pt alloy surfaces, as we shall see in a later section on methanol electrooxidation.

The thermal stability of metal overlayers can be problematic and can limit the temperature range available for reactivity studies. Depending on the thermodynamics of

the metal-metal system, thermal annealing of the overlayer can product interdiffusion resulting in a variety of structures, the two most common structures being a multilayer surface alloy or a single adlayer in equilibrium with a dilute bulk alloy. Overviews on the structure of surface alloy chemistry have been presented by Bardi [23] and Campbell [2]. For some bimetallic systems, this can be a short-cut method for producing a single-crystal alloy surface, avoiding the difficulties that can be encountered in growing a bulk single crystal. However, it is not necessarily the case that the surface alloy produced in this way will have the identical structure to the bulk alloy of (nominally) the same composition, because the latter are non-equilibrium structures. A good example of this is the Sn/Pt(111) system. As shown in the very elegant study by Galeotti et. al. [29], under some conditions of annealing the resulting surface has the same structure as that of $Pt_3Sn(111)$ while at another it has a non-bulk structure. Nonetheless, the surface alloy method of preparation offers many advantages and if a bimetallic surface alloy with particularly interesting catalytic properties is made this way, a bulk alloy crystal can always be grown for further studies.

BIMETALLIC ELECTROCATALYSIS

Oxidation of Adsorbed CO

The anodic oxidation of adsorbed CO, usually by anodic stripping voltammetry, plays a similar role as a "test molecule" in electrocatalysis as it does in gas-phase catalysis. It is, however, misleading and fundamentally incorrect to create an analogy between anodic stripping voltammetry of CO_{ads} and temperature-programmed thermal

desorption (TDS), as is sometimes done. Anodic stripping is not desorption of CO, (although some desorption of CO_{ads} may actually occur, it is a very small fraction of the total CO_{ads}) it is a surface reaction, having the stoichiometry (in acid solution),

$$CO_{ads} + H_2O \Longrightarrow CO_2 + 2\,H^+ + 2\,e^- \qquad \{2\}$$

This reaction has been studied extensively on polycrystalline Pt. An excellent detailed discussion of the charge under the stripping peak, and the relation of that charge to CO coverage, for both polycrystalline Pt and the low-index single crystal faces, was presented by Weaver et. al. [30]. In brief summary, the saturation coverage of CO on Pt surfaces ambient temperature varies from 0.85 to 1.0 CO/Pt surface atom, depending on crystal face. Figure 7a shows the CO stripping voltammetry on sputter-cleaned polycrystalline Pt surface transferred from a UHV chamber, following adsorption of CO at a potential of 0.075 V and subsequent purging of the solution with inert gas (from [31]). The multiplicity of oxidation peaks is usually postulated to derive from oxidation of CO on the different facets of low-index planes present on a polycrystalline Pt surface [32]. In general, the oxidation of an adsorbed monolayer of CO on Pt is understood to proceed along the perimeters of CO islands on the electrode surface, initiating from nucleation sites which facilitate the electrochemical adsorption of oxygen-containing species necessary for the formation of CO_2 [33].

The voltammetry in the pure supporting electrolyte and the CO stripping voltammetry for a CO adsorption potential of 0.075V of sputter-cleaned Ru transferred from UHV is shown in Figure 7b, *i.e.*identical conditions to the Pt voltammetry above. The onset of the CO oxidation current commences at ≈0.25 V, a significantly more

negative potential than for CO on Pt. Similarly, the CO stripping peak on Ru is shifted ≈0.15 V negative compared to Pt, such that the apparent electrocatalytic activity of a Ru electrode is far superior to Pt. It is well known that the adsorption of oxygen-containing species onto a Ru electrode commences at potentials as low as 0.2 V, approximately 0.5 V more negative than on Pt [34]. Thus, oxygen-containing surface species are supplied to a Ru electrode at low potentials, thereby facilitating the onset of the oxidation of CO to CO_2 at a potential significantly more negative than on Pt. The intrinsic reaction rate constant for the reaction of surface-bound species of CO and oxygen, however, seems to be lower as indicated by the greater width of the CO stripping peak on Ru at 20 mV/s (as well as at 5 mV/s).

Figure 8 summarizes exactly equivalent results for the stripping voltammetry of saturated monolayers of CO on Pt-Ru alloy surfaces, prepared and characterized in UHV, and transferred into an electrochemical cell, in 0.5 M H_2SO_4 at a CO adsorption potential of 0.075 V. To afford a more condensed representation, only the anodic currents in the voltammetry of the respective alloys after the stripping of CO are plotted; the CO stripping voltammetry on pure Ru is added for comparison. The Ru **surface concentration** (by LEIS) in atomic fractions for the different bulk alloys is given in the figure. It is clear from Figure that even small amounts of Ru in the alloy surface, *e.g.*≈7 atomic%, effect a substantial enhancement over pure Pt in their electrocatalytic activity towards the oxidation of adsorbed CO (top voltammogram in Figure), indicated by the peak shift of the CO stripping peak to more negative potentials, by roughly 0.18 V. Increasing the surface concentration of Ru on Pt-Ru alloys further improves the

electrocatalytic activity, and the alloy with ≈46 atomic% yields a CO stripping peak 0.25 V more negative than pure Pt. The significant activity enhancement based on the shift in stripping peak potential as a function of Ru surface composition is also manifested by a striking decrease in the corresponding peak widths. More quantitative kinetic data were obtained by potential step measurements, which revealed similar trends in activity with composition. A simple model which explains the maximizing of the activity at ca. 50 % Ru was derived. Initially, CO is adsorbed on both Pt and Ru surface atoms. Following oxidation of the CO adsorbed on Ru sites, the resulting bare Ru surface atoms appear to provide nucleation sites for the adsorption of oxygen-containing species which then can initiate the further electrooxidation of CO adsorbed either on a Pt or a Ru site nearby:

$$Ru + H_2O \longleftrightarrow (OH)_{ads} + H^+ + e^- \qquad \{3\}$$

$$(CO)_{ads} + (OH)_{ads} \xrightarrow{rds} CO_2 + H^+ + e^- \qquad \{4\}$$

The number of nucleation sites for the formations of OH_{ads} species at low electrode potentials will then be roughly proportional to the atomic fraction of Ru in the alloy, effecting a successively more negative CO stripping peak potential as the Ru surface concentration is increased. It is easily shown [31] that the rate of reaction {4}above is maximized when $\Theta_{CO} = \Theta_{OH} = 0.5$, and thus the activity is maximized at a surface composition of 50 %. This model is a variation of the "bifunctional mechanism" proposed some time ago by Watanabe and Motoo [35] for a related but not identical system: CO molecule (dissolved) oxidation on a Pt surface modified by electrodeposited Ru. The variation in the bifunctional mechanism is important, as we shall see later, and essential to understanding the systematic behavior of a variety of Pt bimetallic systems.

In the above model, CO is adsorbed on both Pt and Ru sites, and thus Ru atoms do not serve exclusively to nucleate OH_{ads}, but are also a source of CO_{ads}. I emphasize that this is not a matter of "splitting hairs" or semantics, it is a very fundamental difference. I also point out to electrochemists who my be less familiar with gas-phase catalysis that the concept of bifunctional catalysis is well-established in that field, and pre-dates the appearance of the concept in the electrochemical community by about two decades. An interesting perspective on bifunctionality in bimetallic hydrocarbon catalysis can be found in the monograph by Sinfelt [36].

The intermixing of Pt and Ru surface atoms plays an extremely important role in the electrocatalytic properties of this bimetallic system. This effect can be seen in selected experiments by Gasteiger et. al. (Fig. 8 in ref.31), and perhaps more directly in the ir spectroscopic study of Stimming and co-workers (37a,b). Gasteiger et. al. [31] compared CO stripping voltammetry on two surfaces having (nominally) the same 8 % Ru surface composition but prepared in two different ways, one sputtered-cleaned $Pt_{90}Ru_{10}$ alloy and the other a sputtered then annealed $Pt_{70}Ru_{30}$ alloy. The stripping peak is actually quite different, with the annealed surface having the more positive peak potential. This was attributed to clustering of the Ru atoms in the annealed surface, which is predicted in Monte-Carlo simulations [38] of alloys with slightly endothermic heats of mixing (as is the case for Pt-Ru). Iannielo et.al. (37b) showed that the ir spectra of CO_{ads} on Pt-Ru alloys have a single vibrational (C - O stretch) band whose frequency is in between that of on the pure metals. This is rather easily explained as vibrational coupling between identical states of CO_{ads} , *e.g.* linearly bonded in the a-top sites, on

individual atoms if they are atomically mixed. On the other hand, if there is clustering of Ru atoms, then one expects to see at least two different stretching frequencies for the CO_{ads}. In fact, this is exactly what Friedrich et. al. (37a) reported for Ru electrodeposited on Pt(111) at nominally 0.5 ML coverage, where by STM the Ru is clustered into ca. 3 nm islands. Interestingly, Friedrich et. al. actually found three separate stretching frequencies, corresponding to CO_{ads} on the Ru "islands", on the Pt "ocean", and at the Pt-Ru boundaries (the "beaches"). Thus, one would expect to see fundamentally different catalytic properties of the three differently prepared surfaces of the *same Pt-Ru bimetallic system:* sputtered bulk alloy, annealed bulk alloy, and submonolayer Ru deposited on Pt. We shall see in the subsequent sections that in fact this is the case. There have not been enough studies of the atomic intermixing in bimetallic electrocatalyst surfaces to make a general conclusion about it, simply from looking at the bifunctional mechanism of action one can see that this intermixing is an extremely important fundamental parameter in the catalysis by any bimetallic system.

Ru appears to be unique among the elemental electrode materials in its ability to oxidize CO_{ads} at low potential, *e.g.* below 0.3 V. The other Group VIII metals, such as ir, Os, Rh, or Pd have very Pt-like stripping peak potentials. It is somewhat surprising that Os, immediately below Ru and just to the left of ir in the Periodic Table, is more ir-like than Ru-like in this regard. Since all of these metals adsorb CO quite strongly, this appears to reflect the nucleation of OH_{ads} species on the surface at low potential, consistent with the expectation that as one goes from 3d to 4d to 5d in a given column, the oxophilicity of the metal decreases substantially. Metals to the left of Ru, with the

possible exception of Re, are covered by an oxide film in aqueous solution, and I am not aware of an observable state of CO_{ads} on these surfaces. Re is the possible exception, but I am not aware of any studies of CO adsorption and/or oxidation on pure Re electrodes. The Group I-b metals, Cu, Ag and Au, do not adsorb CO strongly, and there is no anodic stripping peak for these metals in the absence of CO in solution. Elements to the right of Group I-b are either dissolved in the potential region of interest (above 0 V) or are covered by a passive oxide film, *i.e.* they do not adsorb CO strongly, and there is no anodic stripping peak for these metals in the absence of CO in solution.

Bimetallic electrodes composed of Pt and elements to the right of the Group I-b elements have been widely studied, primarily in the form of the ad-metal underpotentially deposited (UPD) on the Pt surface. There are also many reports of activity enhancement for C_1 electrooxidation on Pt surfaces modified in this way. However, the anodic stripping of CO_{ads} is reported for only a select few of these systems, since the potential for oxidizing CO_{ads} is often positive of the potential of deposition. I am not aware of a single published report where an *underpotentially deposited metal adatom* produced a shift in the CO_{ads} stripping peak to lower potential. There are, however, well-known reports by Motoo and Watanabe [36] of enhanced activity for the oxidation of dissolved CO gas (and a number of other C_1 compounds) for Pt electrodes modified by adsorption of Sn and Ge from solution. Even though these reports appeared more than 20 years ago, and were followed by numerous studies by Motoo and Watanabe and by others of C_1 molecule oxidation using these so-called adatom modified surfaces, I am not aware of a single report of a shift in the CO_{ads} stripping peak to lower potential for Pt electrodes

modified by adsorption of Sn and Ge from solution. The reports for each C_1 molecule will be discussed critically in the next sections. In this section, where only the oxidation of adsorbed CO is being discussed, the conclusion is that the $Pt_{50}Ru_{50}$ alloy surface is the most active surface known. It is not then surprising that this same surface is very active (but not always the most active) electrocatalyst for the oxidation of C_1 compounds, since CO_{ads} is an intermediate whose oxidation is, in many instances, the rate limiting step.

Oxidation of Carbon Monoxide (dissolved gas)

Methanol is probably the most studied of the C_1 compounds because of its potential as a logistical fuel and a feedstock for fuel cells. There has also been a kind of folklore in electrocatalysis that a catalyst with high activity for methanol oxidation would also have a high activity for CO oxidation, and vise-versa. Hence, even fundamental research in recent years has tended to focus on methanol electrooxidation. But the practical interest in reformed methanol as a fuel cell feedstock, producing a $H_2/CO/CO_2$ mixture, has rejuvenated the study of CO electrooxidation. One might suspect, from the conclusion of the preceding section, that the $Pt_{50}Ru_{50}$ alloy is the catalyst of choice for CO electrooxidation. It is interesting and informative to understand why this turns out **not** to be the case.

Figure 9 compares the anodic stripping of CO_{ads} with the continuous oxidation of dissolved CO for pure Pt versus $Pt_{50}Ru_{50}$ alloy (for experimental details, see Gasteiger et. al. [39]). Essentially the same catalytic shift between Pt and $Pt_{50}Ru_{50}$ alloy can be observed for the continuous oxidation of dissolved CO as for the anodic stripping of CO_{ads}, with the striking difference that the onsets for continuous oxidation is shifted to

higher potentials by ca. 0.2 V. This shift is due to a negative reaction order with respect to CO partial pressure, *i.e.* the concentration of dissolved CO, which is observed for both pure Pt, pure Ru, and Pt-Ru alloys of any composition [39]. It can be explained quantitatively by a Langmuir-Hinshelwood model for the kinetics; briefly summarizing, negative reaction order results when there is strong adsorption of one reactant with a rate determining step which is a surface reaction between adsorbed species of both reactants, and both reactants compete for the same adsorption sites, *i.e.* CO_{ads} and OH_{ads} compete for the same sites (either Pt or Ru), but CO wins the competition. Thus, the oxidation of CO on Pt-Ru alloy is not a bifunctional mechanism, as suggested in the early work by Motoo and Watanabe [36].

Very different behavior is observed for Pt_3Sn alloys. Detailed results for CO oxidation on Pt_3Sn alloys may be found in the recent papers by Gasteiger et. al. [40a,b]. An overview of these results is shown in Figure 9 . The onset potential for the continuous oxidation of dissolved CO on a sputtered cleaned $Pt_3Sn(110)$ surface is shifted negatively with respect to that for $Pt_{50}Ru_{50}$ alloy by about 0.3 V, and by about 0.45 V with respect to pure Pt. However, the stripping wave for the oxidation of CO_{ads} on $Pt_3Sn(110)$ is in the same potential region as Pt, and is accompanied by Sn-dissolution. Thus, the continuous oxidation of dissolved CO takes place at a high rate, *e.g.*> 0.1 mA/cm^2 and a turnover rate > 1, on a surface *fully covered* by CO_{ads} . The reaction on Pt_3Sn alloys is also strongly structure sensitive, with the potential for the onset of oxidation on the (111) surface shifted lower by about 0.1 V relative to the (110) surface, both surfaces having Sn compositions (by LEIS) of ca. 25 at.%. The mechanism for CO

oxidation on Pt_3Sn alloys has not been established. It is unlikely that CO is adsorbed at Sn sites (it does not do so even in UHV [41]), while it is very likely there is OH_{ads} nucleation at Sn sites, but this has not been observed experimentally. As one might suspect from the foregoing discussion of Pt-Ru alloy, the reaction order on Pt_3Sn alloys is *positive*, about + 0.25. This reaction order would be consistent with an absence of competition between OH_{ads} nucleation and CO adsorption for the same site, so a true bifunctional mechanism, OH_{ads} nucleation at Sn-sites and CO adsorption at Pt-sites, seems likely for this surface. Gasteiger et.al. have proposed [40b] that the uniquely high activity of Pt_3Sn alloy surfaces, and the (111) surface in particular, is due to the formation of a weakly adsorbed state of CO, which is highly mobile on the surface and thus very reactive. Since it is reversibly adsorbed, it is not seen in stripping experiments, which are preceded by purging the cell with inert gas. This weakly adsorbed state of CO is possibly a consequence of the strong intermetallic bonding between Pt and Sn atoms alluded to in the previous section of this chapter. Thus, the Pt_3Sn alloy system is an electrocatalyst having significant implications for both practical use, *e.g.* it is the most active catalyst known for the electrooxidation of CO, and for future fundamental study.

It is at this point interesting to note an intriguing similarity in the electrocatalytic properties of Pt_3Sn(hkl) surfaces and pure Au(hkl) for CO electrooxidation as reported by Weaver and co-workers [42]. Unlike Pt_3Sn(hkl) there is no state of irreversibly adsorbed CO on Au(hkl), but like Pt_3Sn(hkl) there is a reversibly adsorbed state in the presence of CO in solution, observed directly by in-situ FTIR spectroscopy. The oxidation of dissolved CO appears to proceed via this weakly adsorbed state on both surfaces. The

kinetics of oxidation on both have very strong crystal face dependance, but in the case of Au the (111) face is the least active, and the (110) the most active, with a 100-fold difference in rate, a similar difference in rate between $Pt_3Sn(110)$ and (111). The higher rate on Au(110) surface was attributed to the ability of this surface to form an adsorbed state of CO because of the density of "broken bonds" for Au atoms in the fcc(110) rows, i.e. this surface has the highest concentration of weakly bound CO_{ads} . Likewise, the higher activity of $Pt_3Sn(111)$ is attributed to the enhanced formation of weakly bound CO_{ads} on this surface relative to the (110) face. Both surfaces also have positive reaction orders in CO partial pressure, which is also indicative of a reaction pathway via a weakly bound intermediate. The role of OH_{ads} in the reaction is unclear in both cases, and is likely to be very different given the fundamentally different nature of the two surfaces

The potential shifts for the onset of oxidation of dissolved CO on Pt_3Sn alloys reported by Gasteiger et.al. [40a,b] are much larger than the comparable potential shifts reported by Motoo and Watanabe [35] for this reaction on Pt electrodes modified by Sn deposition/adsorption from solution. This is not just a matter of different results from different laboratories; Figure 10 shows results from our laboratory for CO oxidation on a Pt(111) surface modified by Sn deposition/adsorption from solution. Details of the deposition were reported in [43] while the result was presented in [44]. The Sn coverage in the figure is 0.5 Sn per Pt, determined by ex-situ AES, which is the coverage giving the maximum activity. The onset potential for sputter-cleaned $Pt_3Sn(110)$ surface is about 0.15 V lower than that for the Sn-modified Pt(111) surface, corresponding to about 10 times higher activity at 0.45 V; the onset potential for the most active alloy surface,

$Pt_3Sn(111)$, is further shifted by about 0.1 V, being more than 100 times as active as the Sn-modified Pt(111) surface. Note also that the Tafel slope, d ln I/ dV, is significantly different between the alloy and the Sn-modified Pt surfaces, indicating fundamentally different mechanisms for the two surfaces.

There is, in general, a disinclination to publish negative results, except as part of a study of systematic trends in activity with a variation in some characteristic of the catalyst, *e.g.* composition, in which case they are quite valuable. In my laboratory, we have been conducting just such a systematic study, looking at the variation in activity for CO oxidation with $Pt_{75}M_{25}$ alloys, where M are the metals above, below and to the sides of Ru and Sn: Fe, Mo (not Tc), Rh, and Re, and Ge, In, Sb and Pb, respectively. This study is incomplete, so trends are not clear. Pt-Fe and Pt-Ge have poor activity for CO oxidation, the latter being even less active than Pt. We had also studied, earlier, Pt_3Ti, Pt_3Co, and $Pt_{75}Ni_{25}$ alloys. As mentioned in the previous section, these alloys are of interest for the electronic effect, since the clean annealed surface in these alloys is pure Pt. In spite of the fact that the CO_{ads} bond energy is significantly weakened in these alloys (lower by about 20 kJ/mol for Pt_3Ti to about 10 kJ/mol for $Pt_{75}Ni_{25}$, or about 10 - 20 % of the bond energy at low coverage, see [42]) from the intermetallic bonding of the surface Pt atoms to the Ti, Co, Ni atoms in the second layer, the oxidation of CO on these alloys is very Pt-like, as is the anodic stripping peak for CO_{ads}. These negative results are interesting in that they underline the importance of the role of the admetal in the alloy in nucleating OH_{ads} on the surface, and the importance of the bifunctional mechanism in C_1 electrooxidation on bimetallic alloy electrocatalysts. The unique activity of Pt_3Sn

alloy for CO oxidation may be due to an unusual combination of both factors, strong intermetallic bonding producing an electronic effect on the properties of *both* Pt and Sn atoms, plus a bifunctional character as well.

Formic Acid Oxidation

The mechanism of formic acid electrooxidation on Pt and selected Pt-Group metal surfaces in acid solution is reasonably well-established, the so-called "dual-pathway" originally suggested by Capon and Parsons (see [45]),

$$\text{HCOOH} \xrightarrow{\text{dehydrogenation}} CO_2 + 2\,H^+ + 2\,e^- \qquad \{5\}$$

$$\text{HCOOH} \xrightarrow{\text{dehydration}} CO_{ads} + H_2O \qquad \{6\}$$

It would not be an exaggeration to say that the study of this reaction on Pt by *in-situ* IR spectroscopy is one of the most successful uses of spectroscopic methods in modern electrochemistry. These studies are well documented in reviews written by some of the pioneers in this field, Beden and Lamy [46] and Bewick and Pons [47]. For metals other than Pt, however, the number of studies of the intermediates in this reaction by *in-situ* IR spectroscopy is far less. Some studies with Rh are discussed by Beden and Lamy [46]. What these studies have shown is that on pure Pt surfaces at potentials below 0.6, *i.e.* the potential where CO_{ads} is oxidized, the reaction takes place via dehydrogenation on a "CO-poisoned" surface, the CO_{ads} accumulating to some steady-state coverage via the dehydration reaction. Figure 11 shows a characteristic result for pure Pt, and a comparison with a pure Ru surface, from the recent work of Markovic et. al. [48]. The

coverage by CO_{ads} was determined by *in-situ* IR spectroscopy. The interaction of HCOOH with Pt at potentials below 0.2 V is relatively weak, with only a small amount of spontaneous dehydration taking place upon immersion at 0.06 V. Very little current from either the dehydration or dehydrogenation reactions is observed until the potential is scanned above about 0.2 V, where there is the appearance of both and solution phase CO_2. The branching ratio of the dehydrogenation/dehydration reactions was estimated to be about 10^2 in this potential region. Both the anodic current and CO_{ads} coverage reach a plateau on the anodic scan between 0.6-0.7 V. Note that the coverage at this plateau, ca. 0.5 ML, is much lower than the saturation coverage produced by the direct adsorption of CO(gas), which is 0.9 ML (or higher). Above 0.7 V, the oxidation of CO_{ads} produced a large increase in total current and a decrease in CO_{ads} coverage. The large increase in current during the reverse sweep associated with a relatively small reduction in CO_{ads} is indicative of a highly non-linear dependence of the overall rate on CO_{ads} coverage, as inferred from purely kinetic modeling [49]. Briefly restating, the overall reaction of HCOOH on Pt at potentials from 0.2 - 0.7 V is via direct 2 e^- dehydrogenation reaction with from the dehydration reaction acting as a site blocking "poison" rather than a reaction intermediate.

The interaction of HCOOH with a pure Ru surface is a stark contrast to that of Pt. Essentially instantaneous dehydration of HCOOH occurs upon immersion of Ru at 0.06 V leading to a **saturation coverage of CO_{ads} !** No significant production of CO_2 occurs until the potential is scanned above 0.45 V, corresponding to the oxidation of the CO_{ads} as evidenced by the decreased coverage determined by IR spectroscopy. At the potential

where ca. 50 % of the original saturation coverage of CO_{ads} has been oxidized, a current peak is observed which is within 50 mV of the current stripping peak for produced by direct adsorption of CO (Figure 7). At the current plateau at 0.7 - 0.8 V, the CO_{ads} coverage falls to 0, and remains 0 on the negative sweep until the potential is below 0.2 V. In brief, the reaction pathway for HCOOH oxidation on Ru is not via dehydrogenation but by dehydration to form the **intermediate** CO_{ads} , which is subsequently oxidized to CO_2. The overall rate of HCOOH oxidation on pure Ru at 0.5 to 0.7 V is significantly less than on pure Pt, by a factor 10 - 20.

The interaction of HCOOH with the Pt-Ru alloy then becomes an interesting test of the synergistic effect of alloying, *i.e.* unique interactions arising from Pt-Ru site pairs and other ensembles. The most active surface of the Pt-Ru alloys is the 50 % surface, which in the potential region 0.5 - 0.7 V the activity is about 5 times higher than on pure Pt [48]. The enhancement in the rate is due to an enhanced rate of CO_{ads} oxidation at Pt-Ru pair sites, which changes CO_{ads} from a mere spectator species (a poison) to a reaction intermediate [48]. The reaction path on the alloy surface is consequently via both pathways, a true parallel reaction path, but the branching ratio is still very high, *i.e.* Pt-like. The principal effect of opening the dehydration path at steady-state (via the presence of Ru in the surface) is to lower the coverage of CO_{ads} and permit the dehydrogenation path to increase in rate.

It is important to note that in the technologically important potential region of 0 - 0.2 V, Pt and Ru have neither complementary nor synergistic properties which lead to enhanced activity. Pt interacts too weakly with HCOOH in this potential region, and Ru

interacts with HCOOH very strongly but the CO_{ads} which forms cannot be oxidized in this potential region on either surface. Using the simple bifunctional concept, a possibly promising direction of exploration would be Ru-based alloys, seeking an admetal to promote CO_{ads} oxidation in this potential region.

The most widely studied bimetallic catalyst surfaces for HCOOH are not Pt-based alloys, but Pt surfaces modified by electrodeposition (usually in the underpotential region or UPD) of a non-Pt Group element, typically Group 2b, 3,4 and 5a elements. Many examples of these studies (prior to 1988) have already been discussed by Parsons and Vander-Noot [45]. The most frequently cited mechanism of action of these modifiers is a so-called "third-body effect", which is neither well-understood nor means the same thing to different researchers. In essence, in the third-body effect, there is deposition of a inert metal adatom (the third body) which poisons both the dehydrogenation and the dehydration reactions, but in such a way that the poisoning effect of the remaining CO_{ads} plus metal adatom is less than the poisoning produced by the CO_{ads} on the unmodified surface. How is this possible ? The difficulty of envisioning such an effect, and the subtleties involved in modeling it, have made this effect controversial and often misused. Also leading to controversy is the sensitivity of the enhancement by UPD species to differences in experimental conditions, *e.g.* formic acid concentration, potentiodynamic or potentiostatic measurement. Most explanations of the third-body effect in formic acid electrocatalysis are similar to the so-called ensemble effects in hydrocarbon catalysis, although the explanations have rarely been put in that form in the electrochemical literature. One of the rare exceptions is the elegant study by Chang et.al. [49a], who used

in-situ FTIR spectroscopy to study the formation of CO_{ads} on Pt(111) and (100) surfaces modified by Bi adatoms. As I discussed in a previous section, Campbell [2] has shown how an inert metal adatom, Bi, can be used to study the ensemble effect in hydrocarbon dehydrogenation reactions, where there is a critical ensemble of bare Pt atoms needed for H extraction. Translated to the case of HCOOH electrooxidation, if the ensemble of bare Pt atoms required for the dehydration reaction is much higher than that required for the dehydrogenation reaction, then it one might expect that an inert metal adatom would have a net catalytic enhancement. Clavilier et. al. [49b] had previously observed that Bi adatoms had a significant enhancement in the activity of Pt(111) and (100) for formic acid oxidation, which they interpreted as a "third-body effect" versus an OH_{ads} nucleation effect. The IR spectroscopy by Chang et.al. showed directly that Bi reduced the steady-state coverage of CO_{ads}, with the effect being especially dramatic on the (100) surface, where the coverage by CO_{ads} was essentially nil at the optimum Bi coverage. Chang et.al. suggested that this result was consistent with an "ensemble effect" by Bi on the formic acid adsorption/decomposition reactions, with apparently a larger ensemble of contiguous Pt sites required for dehydration than for dehydrogentation. Unless the Bi adatom is totally selective in blocking the dehydration reaction, it is likely that some combination of both effects are at work, *i.e.*the detailed effect of the adatom on *both* reactions and the effect of both the adatom and CO_{ads} on the dehydrogenation reaction. While the study by Chang et.al. is a big step forward in clarifying the "third-body" effect in electrocatalysis, there is still some work to be done. Both Clavilier et.al. and Chang et.al. used Bi deposited by irreversible adsorption from solution, and unlike the UHV

studies cited by Campbell, where the Bi adatoms are known to form ordered superlattices, the structure of the Bi adlayer is not known. The optimum ensemble effect is achieved by atomically dispersed Bi. There is clearly an important role to be played in the future by structure-specific *in-situ* spectroscopies in elucidating these details.

Oxidation of methanol

Sometimes the order in which studies are conducted can work against the evolution of thought in scientific inquiry. I would contend that that is the case in the electrocatalysis of C_1 compounds. The early success of the "dual-pathway" model in explaining the mechanism of formic acid oxidation and providing at least a framework for discussing the enhancements by UPD metals worked against the development of a model for methanol oxidation that was in accord with experiment. An analogous dual-pathway was frequently proposed (see [45] for the history), again with CO_{ads} as a spectator species, *i.e.* a poison, but now from the dehydrogenation reaction, and an unknown intermediate was responsible for the direct oxidation to CO_2, *e.g.*

$$CH_3OH \Longrightarrow ? + H_2O \Longrightarrow CO_2 + 6\,H^+ + 6\,e^- \qquad \{7\}$$

$$CH_3OH \Longrightarrow CO_{ads} + 4\,H^+ + 4\,e^- \qquad \{8\}$$

Much effort, particularly with *in-situ* IR spectroscopy, has been expended in trying to identify this unknown intermediate, and to date none has been identified. In-situ IR spectroscopy has, however, played an extremely important role in refining our understanding of this reaction and in producing a different concept of the role of CO_{ads} in the reaction, namely that of **intermediate** versus poison. As was the case in gas phase

catalysis in the early 1960's, as described by Sinfelt in his monograph [36], the study of the reaction on alloy catalysts has helped to redefine our understanding of the reaction path and the role of CO_{ads} . I will illustrate that with an example of a study conducted in my group in collaboration with Mike Weaver's group using the same Pt-Ru alloys we used previously in the studies of CO_{ads} and dissolved CO(gas) oxidation. First before I do that, let me emphasize that there have been many important studies of methanol adsorption on Pt electrodes by *in-situ* IR spectroscopy which are not discussed in this chapter. These studies have been so extensive, and have such a long history with many twists and turns, that a thorough review of the subject would be a full chapter in itself. There have been far fewer studies of methanol adsorption on bimetallic surfaces using *in-situ* IR spectroscopy, and it is those that I draw upon for the purposes of this chapter.

Figure 12 shows the CO_{ads} coverages on Pt, $Pt_{90}Ru_{10}$ and $Pt_{50}Ru_{50}$ surfaces following immersion at 0.06 V in 0.1 M $HClO_4$ containing 0.05 M methanol. Also shown is the corresponding anodic current as a function of potential. The details are given in [48]. .Only linearly bonded CO_{ads} , as evidenced by the C-O stretch feature at 2040-2080 cm^{-1}, was observed on these surfaces and only CO_2, evidenced by the sharp asymmmetric stretch at 2343 cm^{-1}, was observed in solution as the oxidation product at all potentials, *i.e.* there was no detectable amount of adsorbed formyl species nor were any partial oxidation products such as formic acid or methyl formate observed. Only a single C-O stretch was observed even though the frequencies for pure Pt and pure Ru differ by ca. 50 cm^{-1} . This result is similar to that reported by Ianniello et.al. [37b] for CO_{ads} from direct CO adsorption on the Pt-Ru alloy surfaces, and is attributed to the vibrational

coupling between CO_{ads} molecules adsorbed on adjacent atoms. On the Pt and $Pt_{90}Ru_{10}$ surfaces, a bell-shaped functionality of CO coverage vs. potential is observed with the onset of the ir signal for CO_{ads} at about 0.1 V. No CO_2 is observed until about 0.45 V. All of the current on the first sweep from 0.06 V should then correspond to CO_{ads} formation from the dehydrogenation reaction, and integration of this current was consistent with this result (assuming 4 e^- per CO_{ads}). The onset of methanol oxidation to CO_2 begins at 0.45 V, and is accompanied by a decrease in CO_{ads} coverage. In the potential region between 0.5-0.7 V, the rate of methanol oxidation on the $Pt_{90}Ru_{10}$ surface is more than 30 times that for pure Pt. Referring to Fig. 8, 0.5 V is exactly the potential where CO_{ads} begins to be oxidized on the Pt-rich surfaces, giving indication that is an **intermediate** in the reaction. Referring again to our previous discussion of CO_{ads} oxidation, the rate of this step is maximized at 50 % Ru, and thus we should expect a significant lowering of the CO_{ads} coverage on this surface. The CO_{ads} coverage observed on this surface is more than significantly lowered, the coverage is below 0.1 ML (!). These results point to a series mechanism,

$$CH_3OH \overset{k_1}{\Longrightarrow} CO_{ads} + 4\,H^+ + 4\,e^- + H_2O \overset{k_2}{\Longrightarrow} CO_2 + 6\,H^+ + 6\,e^- \qquad \{9\}$$

In spite of the fact that the 50 % Ru surface is essentially free of adsorbed intermediates, *i.e.*"unpoisoned" in the language of the dual-pathway, it is not the most active surface, the 7-10 % Ru surface is the most active. If one takes into account that methanol adsorption

does not occur on Ru sites, then the series pathway helps us understand the way Ru alters the balance between the relative rates k_1 and k_2. Increasing Ru content in the surface increases k_2 (we new that from before), which is maximized at 50 % Ru, but decreases k_1. The fact that CO_{ads} coverage is relatively high on Pt-rich surfaces but falls to near zero for 50 % Ru suggests that there is transition in the rate determining step with increasing Ru content, from the oxidation of CO_{ads} (k_2) to the adsorption/dehydrogenation of methanol (k_1).

Gasteiger et.al. [50] used this series pathway to develop a quantitative model of the dependance of the oxidation rate on the Ru content in the surface. This model is summarized in Figure 13. A bifunctional role of Pt and Ru atoms was assumed, with methanol adsorption/dehydrogenation occuring at an ensemble of Pt atoms and OH_{ads} nucleation occuring at Ru sites. Using statistical analysis, it was shown that the maximum concentration of active ensembles, viz. three-fold Pt sites adjacent to exactly one Ru atom, occurs near 10 % Ru, exactly where the maximum in rate is observed. Further support for the model was found in experiments conducted at higher temperature [51], where it was found that methanol adsorption/dehydrogenation occurs on Ru sites as well as on Pt sites, and that the maximum in total rate moves to higher Ru content, towards 50 %. This shift towards 50 % Ru as the most active surface is consistent with the change in ensemble configuration, where now (at higher temperature) any three surface sites can serve to dehydrogenate methanol, and the rate determining step becomes the oxidation of CO_{ads} for all surface compositions. The most active surface for this step is, as we saw before, $Pt_{50}Ru_{50}$.

While this reaction path and the ensemble model of Gasteiger et.al. provide a reasonable explanation for the role of Ru in enhancing the activity of Pt for methanol oxidation, there is still much to be learned about this reaction on Pt surfaces, to say nothing of other Pt-Group metals and their alloys. The most obvious deficiency in our knowledge remains the dehydrogenation/adsorption reaction, which is not really a single-reaction step, but has a great deal of chemistry buried in it. Pure Pt is the most active surface known for this reaction, which has been studied extensively over a more than 30 year period, from the classic work of Breiter [52] and Bagotzky [53] to very recent studies with Pt single crystal surfaces [54]. As one can see from the latest work, the details are still unresolved, but there has been both progress and a consolidation of ideas. There is appears to be consistent support for the sequence of steps originally but forth by Bagotzky: that three hydrogens are extracted on a bare Pt surface very rapidly, possibly in a concerted manner, without forming or even going through a methoxy intermediate. The ensemble of three Pt sites proposed by Gasteiger et.al. would be consistent with a concerted mechanism. The removal of the fourth hydrogen seems to be slower, possibly explaining the appearance of an adsorbed formyl (HCO) intermediate [*e.g.*ref. 55]. Why this 3 e^- intermediate is seen, *e.g.*with IR spectroscopy, by some groups and not others is not clear, but appears to be from a combination of experimental procedure (especially time effects) and the spectrometer being used. This picture would also be consistent with the general experience that the deposition of inert adatoms on the surface of Pt, even at coverages as low as 0.1 ML, block the production of CO_2 almost completely, producing partial oxidation products like methyl formate and formic acid. Another important aspect

of the detailed chemistry of dehydrogenation on Pt that was controversial for a long time was the potential dependence, in particular, the potential where methanol dehydrogenation begins. It is now certain, as indicated in Figure 11, that in the potential region where there is nearly a monolayer of H_{ads} on the Pt surface, 0 - 0.1 V, there is **no dehydrogenation** (or adsorption) of methanol. This implies that methanol cannot compete with $H_9O_4^+$ for the Pt surface sites in this potential region, *i.e.* formation of H_{upd} is the preferred process.

The series reaction pathway together with current knowledge of the dehydrogenation reaction on Pt provide a sound framework both for further fundamental study and for practical development of methanol oxidation catalysts. With respect to the latter, the Pt-Ru alloy remains the active known catalyst for methanol oxidation in spite of more than 20 years of study of alternative catalysts since the seminal study of Pt bimetallic catalyst by the group at Batelle [1]. These studies have included, at one time or another, the modification of the Pt surface by electrodeposition (usually by UPD) and/or adsorption from solution of nearly every element in the periodic table that can be deposited in this manner. There is only one of these systems which has proven to have any significant **stable** enhancement of the activity of the Pt surface, and that is Sn. Sn adsorbed on Pt from solution has a higher activity for methanol oxidation than the alloy Pt_3Sn [43], the latter actually being **less active** than Pt [43,56]. The enhancement with Sn/Pt is significantly less than with Pt-Ru alloy, but is of fundamental interest. As with Pt-Ru at 298°K, the enhancement is maximized at a very low coverage of Sn, consistent with an absence of adsorption of methanol on Sn adatoms and the analogous (to Ru)

blocking effect of Sn on the Pt ensemble needed for dehydrogenation when the coverage exceeds about 0.1 ML. But it is not clear what role the adsorbed Sn plays in oxidation of the CO_{ads} formed from methanol. Recall from the previous sections that adsorbed Sn has no effect on the oxidation of CO_{ads} produced by adsorption from CO(gas), but does have some positive effect on the rate of oxidation of dissolved CO(gas). There are differences in the nature of CO_{ads} produced from the two sources: the coverage from methanol dehydrogenation is much lower, and the distribution of linearly bonded, bridge bonded and multiply bonded states is much different. A very similar predicament is posed by the relative inactivity of Pt_3Sn for methanol oxidation [57]. Recall from the previous section that the potential for the onset of oxidation of dissolved CO(gas) is more than 0.4 V below the potential for the onset of oxidation of CO_{ads} . The high rate of CO(gas) is attributed, by inference, to a unique state of on Pt_3Sn that does not occur on Pt and is not produced by methanol dehydrogenation on either surface [57]. As I said before, the Pt-Sn system is both technologically promising, but also fundamentally puzzling. Resolving the puzzle will go a long way towards developing new catalysts for methanol oxidation.

The fundamental studies of methanol oxidation, while they have not yet produced new catalysts, have revealed some important lessons for catalyst development. The very strong ensemble effect observed with Ru and Sn means that one needs to control the surface composition when exploring new systems, which is why I put so much emphasis in this chapter on surface analysis and the science of surface enrichment. It is possible that some promising systems have been missed because there was too much of the admetal present on the surface.

CONCLUDING REMARKS

As in heterogeneous catalysis, the use of modern methods of surface analysis has produced a significant growth in our understanding of the mechanism of action in bimetallic electrocatalysts. The ability to tailor-make a controlled and well-characterized arrangement of the two elements in the electrode surface and even near-surface region presages a new era of advances in our knowledge of bimetallic systems. While it is not possible, and probably futile, to completely distinguish "electronic effects" from "ensemble effects", recent studies using well-characterized bimetallic surfaces clearly reinforce the importance of ensemble effects in C_1 electrooxidation, particularly in the case of methanol, where the effect has been relatively neglected. *In-situ* IR spectroscopy has further refined our understanding of the role of CO_{ads} in C_1 electrooxidation, which can be **either** a poison or an intermediate. While there is a significant circumstantial evidence to support the bifunctional mechanism of action in many bimetallic catalysts, compelling evidence can probably only come from new *in-situ* spectroscopies that can reveal the chemistry of the oxidizing species, e.g. OH_{ads} chemistry.

Acknowledgment

The author is pleased to acknowledge the continuing financial support for our research in electrocatalysis from the Assistant Secretary for Energy Efficiency and Renewable Energy, Office of Transportation Technologies, of the U.S. Department of Energy

REFERENCES

1. Binder, H., Koehling, A., and Sandstede, G., In "From Electrocatalysis to Fuel Cells", Sandstede, G., ed., University of Washington Press, Seattle WA, 1972, p. 43ff.
2. Campbell, C.T., *Annu. Rev. Phys. Chem.*, **1990,** *41*, 775.
3. "Surface Segregation Phenomena", Dowben, P.A., and Miller, A. eds., CRC Press, Boca Raton FL, 1990.
4. Sachtler, W.M.H., and Van Santen, R.A. *Adv. Catal.*, **1977,** 26, 69.
5. Chelikowski, J.R., *Surf. Sci.*, **1984,** *139*, L197.
6. Watson, P.R., Van Hove, M.A. and Herman, K. "Atlas of Surface Structures: Volume 1A", Monograph #5, ACS Publications, Washington DC, 1995.
7. Heiland, W. and E. Taglauer, "Ion Scattering and Secondary Ion Mass Spectroscopy", In *Methods of Experimental Physics*, Volume 22, Solid State Physics: Surfaces, Park, R.L. and Lagally, M. eds. Academic Press, Orlando FL,1985, pp. 299-347.
8. Baun, W.L., in "Quantitative Surface Analysis of Materials", ASTM STP 643, McIntyre, N.S. ed. ASTM, Metals Park OH, 1978, p. 150.
9. Gasteiger, H.A., Ross, P.N. and Cairns, E.J. *Surf. Sci.*, **1993,** *293*, 67.
10. Watson, P.R., *J. Phys. Chem. Ref. Data*, J. **1990,** *19*, 85.
11. DeTemmerman, L., Creemers, C., Van Hove, M., Neyens, A., Bertolini, J. and Messardier, J. *Surf. Sci.* **1986,** *178*, 888.
12. Gauthier, Y., Y. Joly, R. Baudoing, and J. Rundgren *Phys. Rev. B* **1985,** *31*, 6216.
13. Abraham, F.F., *Phys. Rev. Lett.* **1981,** *46*, 546.
14. Treglia, G. and Legrand, B. *Phys. Rev. B*, **1987,** *35*, 4338.

15. Kelley, M. and Ponec, V. *Prog. Surf. Sci.* **1981**, *11*, 139.

16. King, T.S., in "Surface Segregation Phenomena", Dowben, P.A., and Miller, A. eds., CRC Press, Boca Raton FL, 1990, pp. 27-77.

17. Mazurowski, J. and P.A. Dowben, In "Surface Segregation Phenomena", Dowben, P.A., and Miller, A. eds., CRC Press, Boca Raton FL, 1990, pp.365-421.

18. Mukherjee, S. and Moran-Lopez, J.L. *Surf. Sci.* **1987**, *189/190*, 1135.

19. Foiles, S., in "Surface Segregation Phenomena", Dowben, P.A., and Miller, A. eds. CRC Press, Boca Raton FL, 1990, pp. 79-107.

20. Foiles, S., Baskes, M.I. and Daw, M.S. *Phys. Rev. B* **1986,** *33*, 7983.

21. Ferro, R., R. Capelli, A. Borsese, and S. Delfino, *Atti. Accad. Naz. Lincei Red. Cl. Sci. Fis. Mat. Nat.* **1973**, *54*, 634.

22. Haner, A.N., Ross, P.N. and Bardi, U. *Catal. Lett.* **1991**, *8*, 1; Haner, A.N., Ross, P.N. and Bardi, U. *Surf. Sci.* **1991**, *249*, 15; Bardi, U., Pedocchi, L., Rovida, G., Haner, A.N. and Ross, P.N. In "Fundamental Aspects of Heterogeneous Catalysis", Brongersma, H.H. and Van Santen, R.A. eds. Plenum, New York, p. 393-7; Atrei, A., Bardi, U., Torrini, M., Zanazzi, E., Rovida, G. and Ross, P.N. *Phys. Rev.B*, **1992**, *68*, 1649.

23. Bardi, U., *Repts. Prog. Phys.*, **1994,** *57*, 939.

24. Bardi, U., and Ross, P.N., *Surf. Sci.* **1984,** *146*, L555; Bardi, U., Dahlgren, D. and Ross, P.N. *J. Catal.* **1986,** *100*, 196.

25. Paul, J., Cameron, S.D., Dwyer, D.J. and Hoffman, F.M. *Surf. Sci.* **1986,** *177*, 121

26. Atrei, A., Pedocchi, L., Bardi, U., Rovida, U., Torrini, U., Zanazzi, E., Van Hove, M. and Ross, P.N. *Surf. Sci.,* **1992,** *261*, 64; Chen, W., Paul, J., Barbieri, A., Van Hove, M.A., Cameron, S.D. and Dwyer, D.J. *J. Phys. Cond. Matter*, **1993,** 5, 4585.

27. Spencer, M.S., *Surf. Sci.*, **1984,** *145*, 145.

28. Rodriguez, J. and Goodman, D. W., *J. Phys. Chem.* **1991,** *95*, 4196.

29. Galeotti, M., Atrei, A., Bardi, U., Rovida, G. and Torrini, M. *Surf. Sci.* **1994,** *313*, 349.

30. Weaver, M., Chang, S.-C., Leung, L.-W., Jiang, X., Rubel, M., Szklarczyk, M., Zurawski, D., and Wieckowski, A., *J. Electroanal. Chem.* **1992,** *327*, 247.

31. Gasteiger, H., Markovic, N., Ross, P. and Cairns, E. *J. Phys. Chem.* **1994,** *98*, 617.

32. De Becdelievre, A., de Becdelievre, J. and Clavilier, J. *J. Electroanal. Chem.* **1990,** *294*, 97; Beden, B., Lamy, C., Tacconi, N., Arvia, A., *Electrochim. Acta* **1990,** *35*, 691.

33. Corrigan, D. and Weaver, M. *J. Electroanal. Chem.* **1988,** *241*, 143; Kunimatsu, K., Shimazu, K. and Kita, H. *J. Electroanal. Chem.* **1988,** *256*, 371.

34. Hadzi-Jordanov, S., Angerstein-Kozlowska, H., Vucovic, M. and Conway, B. *J. Electrochem. Soc.* **1978,** *125*, 1471.

35. Watanabe, M., and Motoo, S. *J. Electroanal. Chem.* **1975,** *60*, 267.

36. Sinfelt, J., "Bimetallic Catalysts: Discoveries, Concepts and Applications", John Wiley and Sons, Inc, New York, 1983, pp. 133-38,

37a. Friedrich, K., Geyzers, K.-P., Linke, U., Stimming, U. and Stumper, J. *J. Electroanal. Chem.* **1996,** *402*, 123

37b. Ianniello, R., Schmidt, V., Stimming, U., Stumper, J. and Wallau, A. *Electrochim. Acta.* , **1994,** *39*, 1863.

38. Vurens, G., Van Delft, F. and Nieuwenhuys, B. *Surf. Sci.* **1987**, *192*, 438.

39. Gasteiger, H., Markovic, N. and Ross, P. *J. Phys. Chem.* **1995**, *99*, 16757.

40a. Gasteiger, H., Markovic, N. and Ross, P. *J. Phys. Chem.* **1995**, *99*, 8945.

40b. Gasteiger, H., Markovic, N. and Ross, P. *Catal. Lett.*, **1996**, *36*, 1.

41. Haner, A. Ross, P., Bardi, U. and Atrei, A. *J. Vac. Sci. Technol. A* **1992**, *10*, 2718.

42. Ross, P., *J. Vac. Sci. Technol. A* **1992**, *10*, 2546

43. Haner, A. and Ross, P. *J. Phys. Chem.* **1991**, *95*, 3740.

44. K. Wang, Gasteiger, H., Markovic, N. and Ross, P. *Extended Abstracts*, 46th Annual Meeting of the International Society of Electrochemistry (ISE), Xiamen, China, 1995, paper no. 1-51.

45. Parsons, R. and VanderNoot, T. *J. Electroanal. Chem.* **1988**, *257*, 9 and references therein.

46. Beden, B. and Lamy, C. In "Spectroelectrochemistry, Theory and Practice", Gale, R. J. ed., Ch. 5, Plenum Press, New York, 1988.

47. Bewick, A. and Pons, B. In "Infrared and Raman Spectroscopy", Clark, R. and Hester R. eds., Vol. XII, Ch.1, Wiley Heyden, London, 1985.

48. Markovic, N., Gasteiger, H., Ross, P., Jiang, X., Villegas, I. and Weaver, M. *Electrochim. Acta* **1995**, *40*, 91.

49a. Chang, S.-C., Ho, Y. and Weaver, M., *Surf. Sci.* **1992**, *265*, 81.

49b. Clavilier, J., Fernandez-Vega, A., Feliu, J., and Aldaz, A. *J. Electroanal. Chem.* **1989,** *258*, 89; *J. Electroanal. Chem.* **1989,** *261*, 113

50. Gasteiger, H., Markovic, N., Ross, P. and Cairns, E. *J. Phys. Chem.*, **1993,** *97*, 12020.

51. Gasteiger, H., Markovic, N., Ross, P. and Cairns, E. *J. Electrochem. Soc.* **1994,** *141*, 1795.

52. Breiter, M. *J. Electroanal. Chem.* **1967,** *14*, 407; *J. Electroanal. Chem.* **1967,** *15*, 221.

53. Bagotsky, and Skundin, A. "Chemical Power Sources", Academic Press, New York, 1980.

54. Herrero, H., Franaszczuk, K., and Wieckowski, A. *J. Phys. Chem.* **1994,** *98*, 5074.

55. see Matsuda, S., Kitamura, F., Takahashi, M. and Ito, M. *J. Electroanal. Chem.* **1989,** *274*, 305 or Lopes, M., Fonseca, I., Olivi, P., Beden, B., Hahn, H., Leger, J., and Lamy, C. *J. Electroanal. Chem.* **1993,** *346*, 415.

56. Campbell, S. and Parsons, R. *J. Chem. Soc. Faraday Trans.* **1992,** *88*, 833.

57. Wang, K., Gasteiger, H., Markovic, N. and Ross, P. *Electrochim. Acta* **1996,** *41*, 2587.

Figure Captions

Figure 1. Schematic diagram of the low energy ion-scattering (LEIS) method for determining surface composition. M_o is the mass of the ion, E_o is the energy of the incident ion beam, E' is the energy of the scattered ions of mass M_o, M_s is the mass of the scattering atom at the surface, and θ is the scattering angle.

Figure 2. LEIS spectrum from an annealed $Pt_{70}Ru_{30}$ alloy surface using a 2 keV $^4He^+$ ion beam (18 nA/cm^2 rastered over an area of 3 mm x 3 mm). Calculated values of E_1/E_o for Pt and Ru atoms are 0.936 and 0.881, respectively. Circles are experimental data, solid lines are fitted using Gaussian line shapes and calculated values of E_1. from [9].

Figure 3. Experimental surface compositions of annealed Pt-Ru alloys versus predictions from a thermodynamic model for different low index planes: (——) fcc(111) and hcp(0001); (- ¨ - ¨ -) fcc(110) and hcp(11-20); (-----) fcc(100) and hcp(10-10); (\\\\\\\) indicates two-phase region of the bulk alloy.

Figure 4. Compositional oscillation at the (111) surface of $Pt_{50}Ni_{50}$ and $Pt_{78}Ni_{22}$ by LEED crystallography. from [14].

Figure 5. Theoretical predictions of surface segregation in Pt-rich binary alloys.

Figure 6. Models of the $L1_2$ fcc structure of Pt_3Sn showing the bulk termination planes of the three low-index faces.

Figure 7. CO stripping voltammetry of UHV sputter cleaned electrodes in 0.5 M H_2SO_4 on (a) Pt and (b) Ru: (—) stripping of a monolayer of CO in the first positive-going sweep; (----) first negative-going sweep after CO stripping, followed by a positive-going sweep. Conditions: 20 mV/s, adsorption at 0.025 V (nhe). from [31].

Figure 8. CO stripping voltammetry of UHV sputter cleaned Pt-Ru alloy and pure Ru electrodes in 0.5 M H_2SO_4 : (—) stripping of a monolayer of CO in the first positive-going sweep; (----) first negative-going sweep after CO stripping. Ru surface compositions determined by LEIS are indicated in the figure in atomic fractions. Conditions: 20 mV/s, adsorption at 0.025 V (nhe). from [31].

Figure 9. Base voltammogram (·····), CO stripping voltammogram (—), and anodic oxidation of dissolved CO in an RDE configuration for UHV sputter cleaned electrodes: (a) Pt-Ru alloy with a surface composition of 50 %; (b) $Pt_3Sn(110)$ with a surface composition of 20 % Sn. (c) and (d) show one-time CO stripping on a expanded potential scale.

Figure 10. Anodic oxidation of dissolved CO on electrodes in a RDE configuration:

(—) UHV sputter cleaned $Pt_3Sn(110)$ with a surface composition of 20 % Sn

(·····) UHV sputter cleaned Pt-Ru alloy with a surface composition of 50 %;

(-----) a UHV sputter cleaned Pt(111) surface modified by 0.5 ML of UPD Sn;

(-·-·-) UHV sputter cleaned Pt(111). Insert shows just anodic sweeps in the low potential region.

Figure 11. (bottom) CO coverages from *in-situ* IR spectroscopy and (top) corresponding cyclic volatmmetry (2 mV/s) of UHV sputter cleaned (a) Pt and (b) Ru electrodes in 0.1 M HClO4 with 0.5 M HCOOH. (·····) base voltammogram without HCOOH. The electrodes were contacted at 0.06 V (nhe). The insert shows the voltammetry of Pt with a magnification of the current in the low potential region. from [48].

Figure 12. . (bottom) CO coverages from *in-situ* IR spectroscopy and (top) corresponding cyclic volatmmetry of UHV sputter cleaned Pt-Ru alloys with(a) $x_{s,o}$ ≈10 at. % Ru and (b) $x_{s,o}$ ≈ 50 at. % Ru surface composition electrodes in 0.1 M HClO4 with 0.05 M CH_3OH. (·····) base voltammogram without CH_3OH. CO coverages on pure Pt (----) shown for reference. The electrodes were contacted at 0.06 V (nhe). The inserts show the voltammetry with a magnification of the current in the low potential region. from [48].

Figure 13. (a) Schematic representation of UHV sputter cleaned Pt-Ru alloy surfaces with 10 and 50 at. % Ru. (b) Geometric arrangement of atoms around a 3-fold methanol adsorption site for an fcc (111) face. (c) Probability distribution for the occurance of a 3-fold Pt site surrounded by exactly one Ru atom for different low-index fcc face geometries as a function of Ru surface composition. from [50].

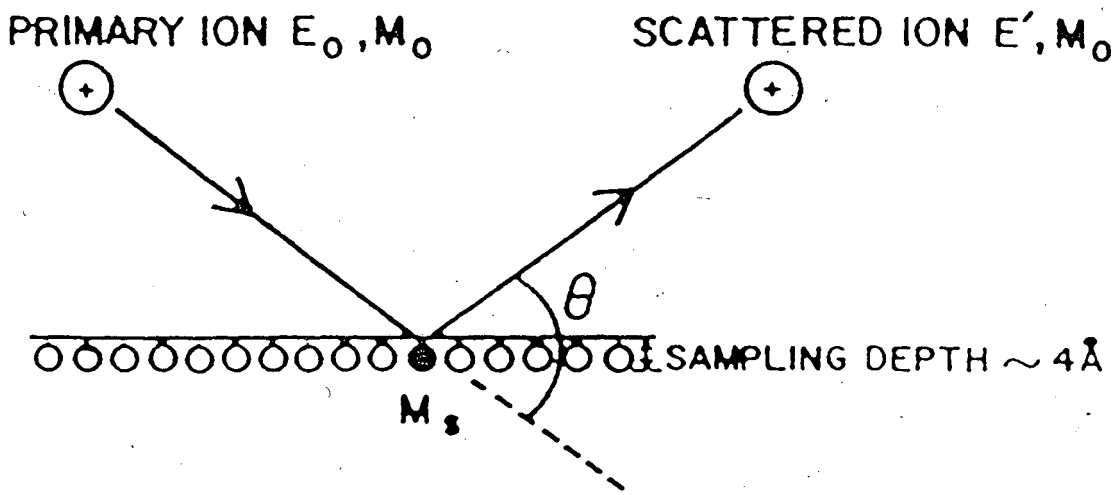

$$\frac{E'}{E_0} = \frac{M_0^2}{(M_0 + M_s)^2} \left\{ \cos\theta + \left(\frac{M_s^2}{M_0^2} - \sin^2\theta \right)^{1/2} \right\}^2$$

Fig. 1

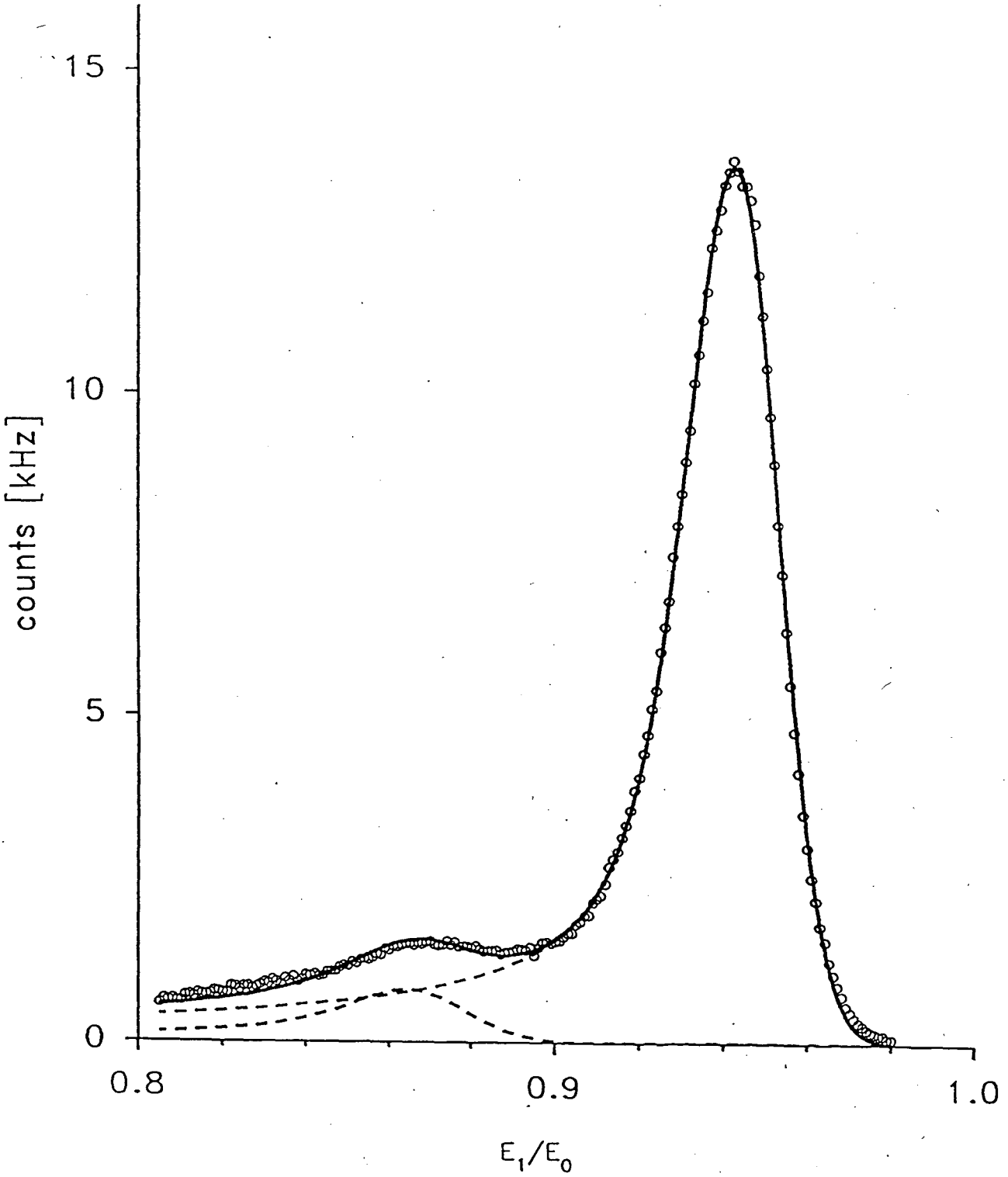

Fig. 2

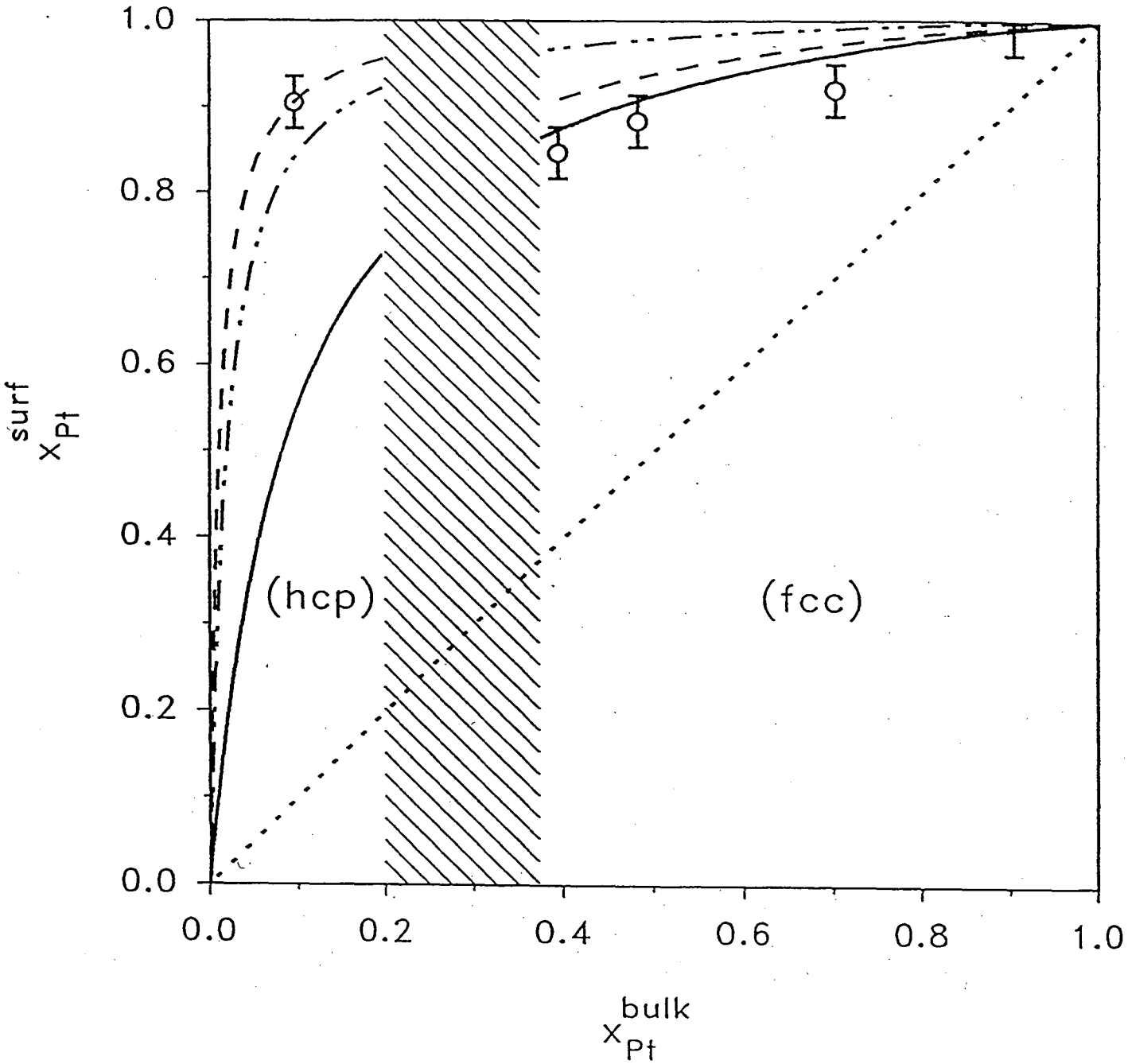

Fig. 3

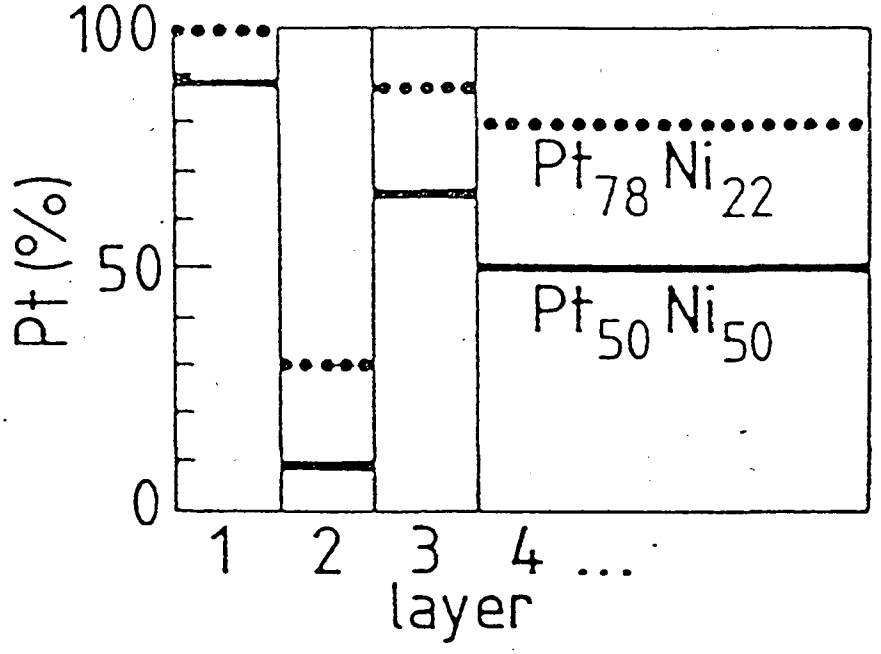

Fig. 4

THEORETICAL PREDICTIONS OF SURFACE SEGREGATION IN Pt-RICH (Pt Solvent) ALLOYS

	Solute element	Enriched in Pt	Enriched in Solute	Theory	Experiment
	Ti	X		[18]	Yes [25,26]
	V	X		[18]	Yes [17]
	Cr	X		[18]	Yes [17]
3d	Fe	X		[18]	Yes [17]
	Co	X		[18]	Yes [17]
	Ni	X		[14]	Yes[12]
	Cu		X	[19,20]	--
	Zr	X		[18]	--
	Nb	X		[18]	--
	Mo	X		[18]	--
4d	Ru	X		[9, 18]	Yes [9]
	Pd	X		[18]	? [17]
	Ag		X	[19,20]	Yes [17]
	Sn		X	[22]	Yes [22]
	Hf	X		[18]	--
	Ta	X		[18]	--
	W	X		[18]	No [17]
5d	Re	X		[18]	No [17]
	Os	X		[18]	--
	Ir	X		[18]	--
	Au		X	[19,20]	Yes [17]

Yes = experiment in agreement with theoretical prediction
No = experiment is not in agreement with theoretical prediction
? = experimental results are contradictory

Fig. 5

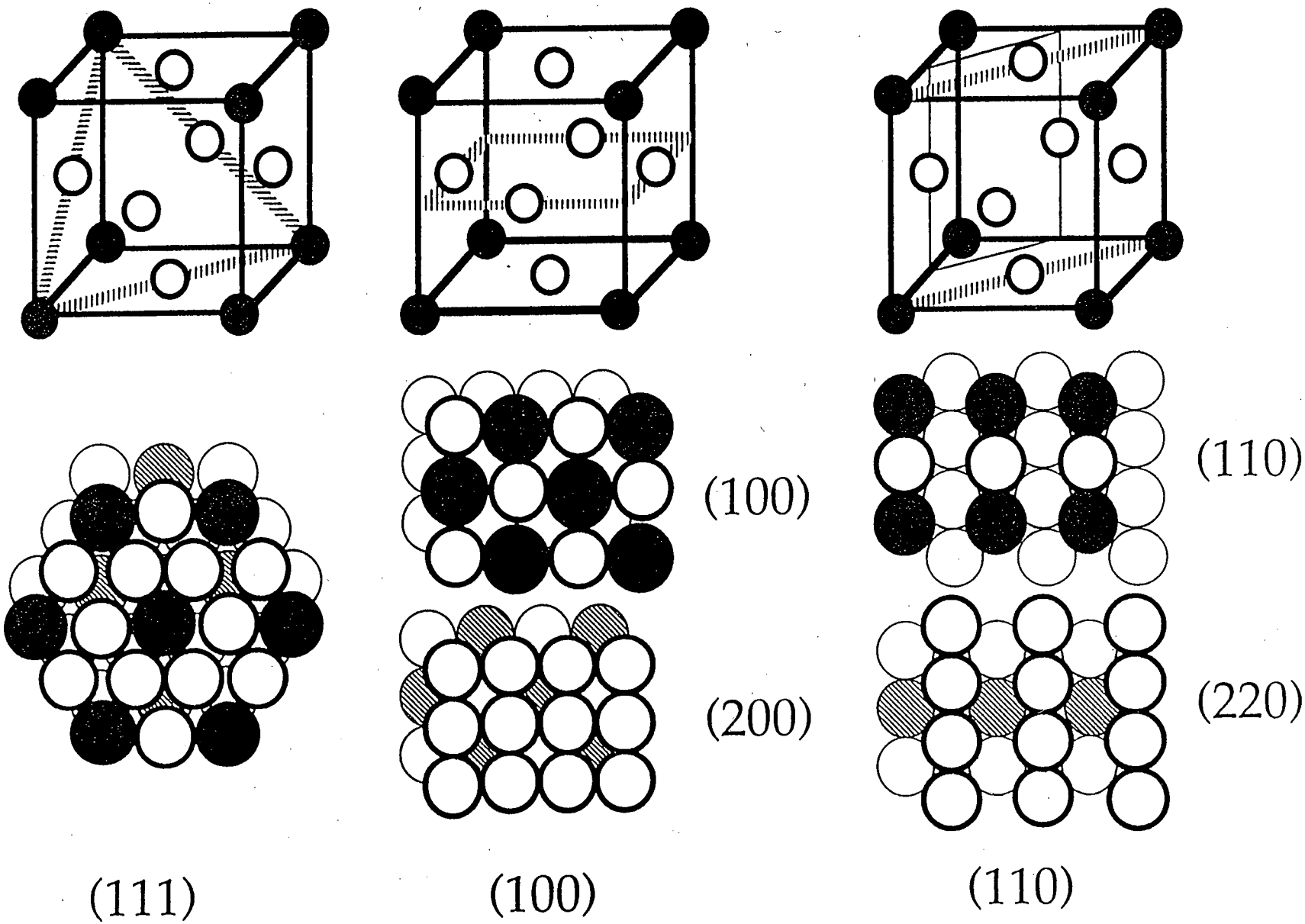

Pt_3Sn

Fig. 6

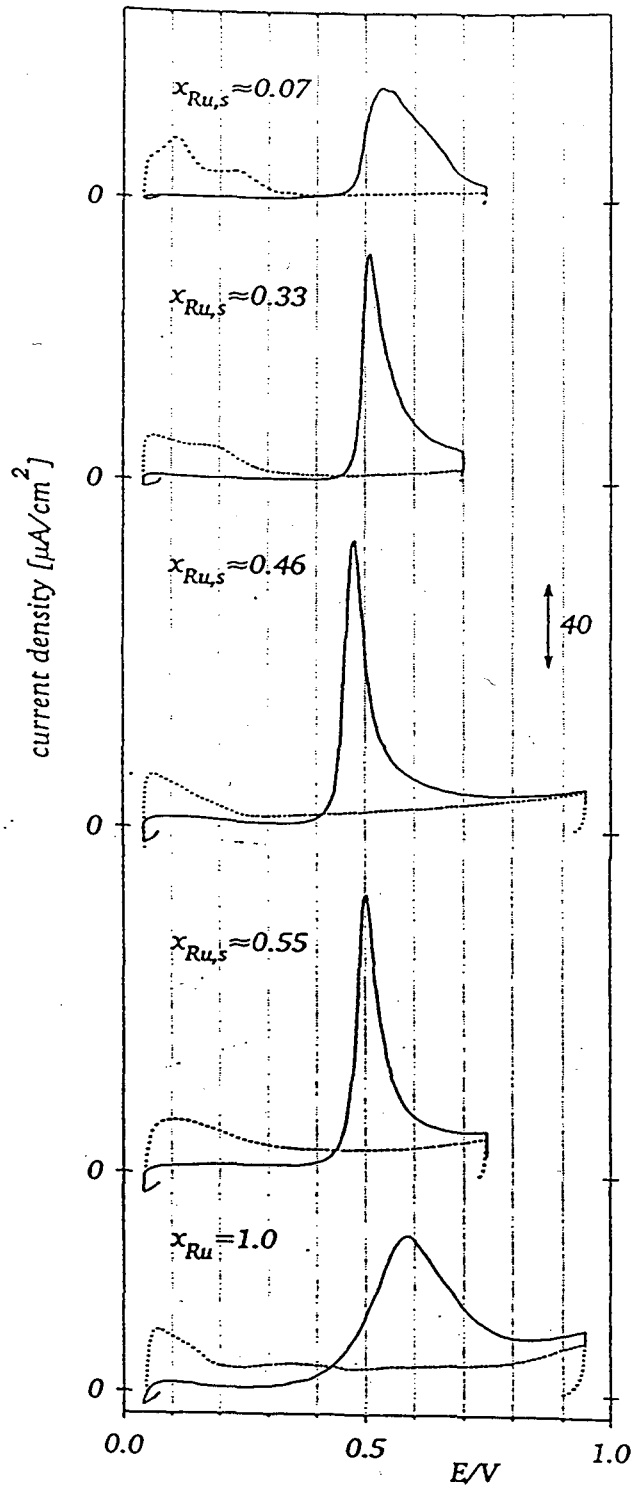
$x_{Ru,s}$≈0.07
$x_{Ru,s}$≈0.33
$x_{Ru,s}$≈0.46
$x_{Ru,s}$≈0.55
x_{Ru}=1.0
0
0
0
0
0
40
current density [μA/cm²]
0.0
0.5
1.0
E/V

Fig. 7

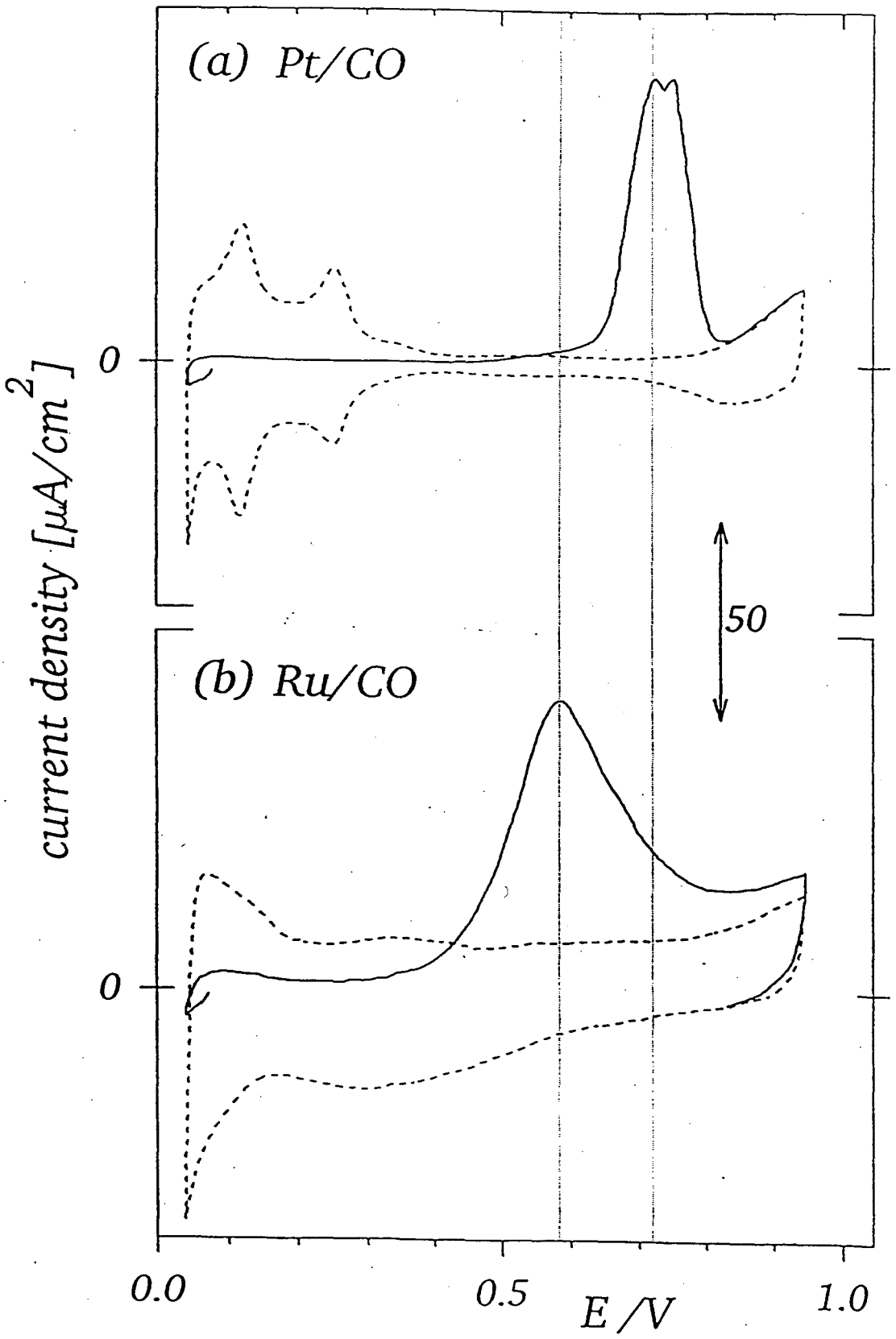

Fig. 8

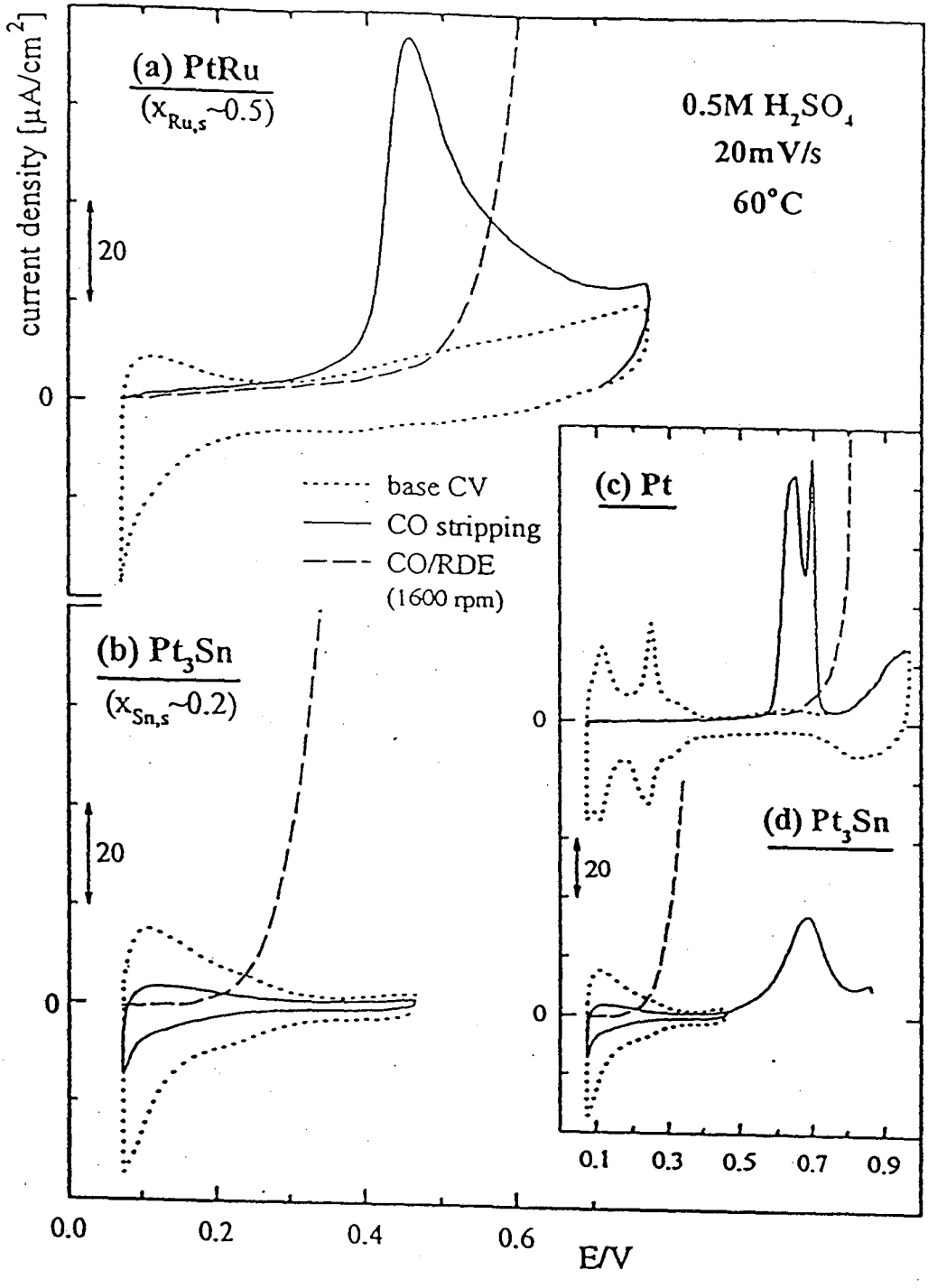
current density [μA/cm²]
(a) PtRu
(x_Ru,s~0.5)
0.5M H₂SO₄
20mV/s
60°C
20
0
base CV
CO stripping
CO/RDE
(1600 rpm)
(b) Pt₃Sn
(x_Sn,s~0.2)
20
0
(c) Pt
0
(d) Pt₃Sn
20
0
0.1
0.3
0.5
0.7
0.9
0.0
0.2
0.4
0.6
E/V

Fig. 9

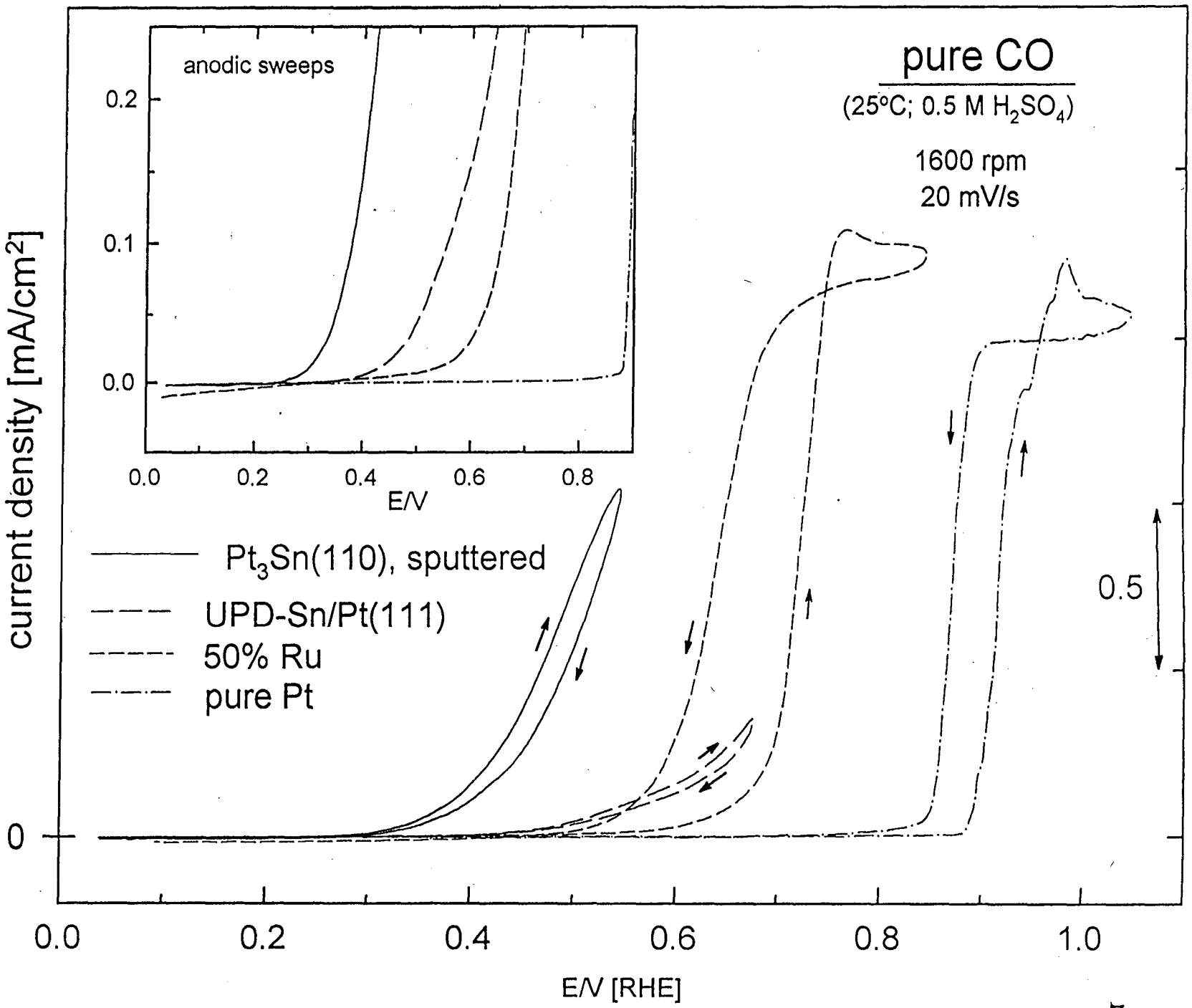
pure CO
(25°C; 0.5 M H_2SO_4)
1600 rpm
20 mV/s
anodic sweeps
0.2
0.1
0.0
0.0
0.2
0.4
0.6
0.8
E/V
current density [mA/cm²]
$Pt_3Sn(110)$, sputtered
UPD-Sn/Pt(111)
50% Ru
pure Pt
0.5
0
0.0
0.2
0.4
0.6
0.8
1.0
E/V [RHE]

Fig. 10

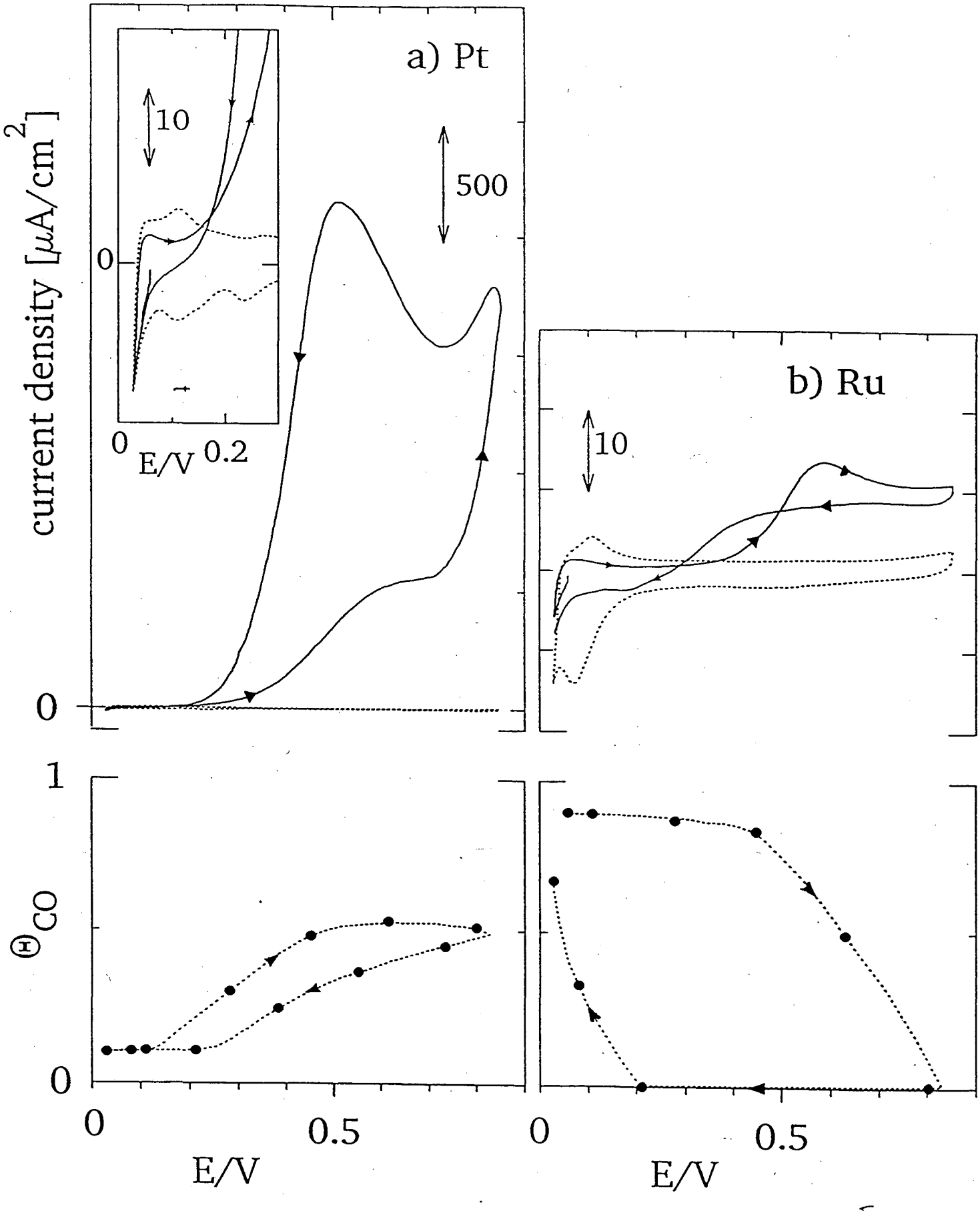
a) Pt
10
500
0
0
E/V
0.2
current density [μA/cm²]
0
b) Ru
10
1
Θ_CO
0
0
0.5
E/V
0
0.5
E/V

Fig. 11

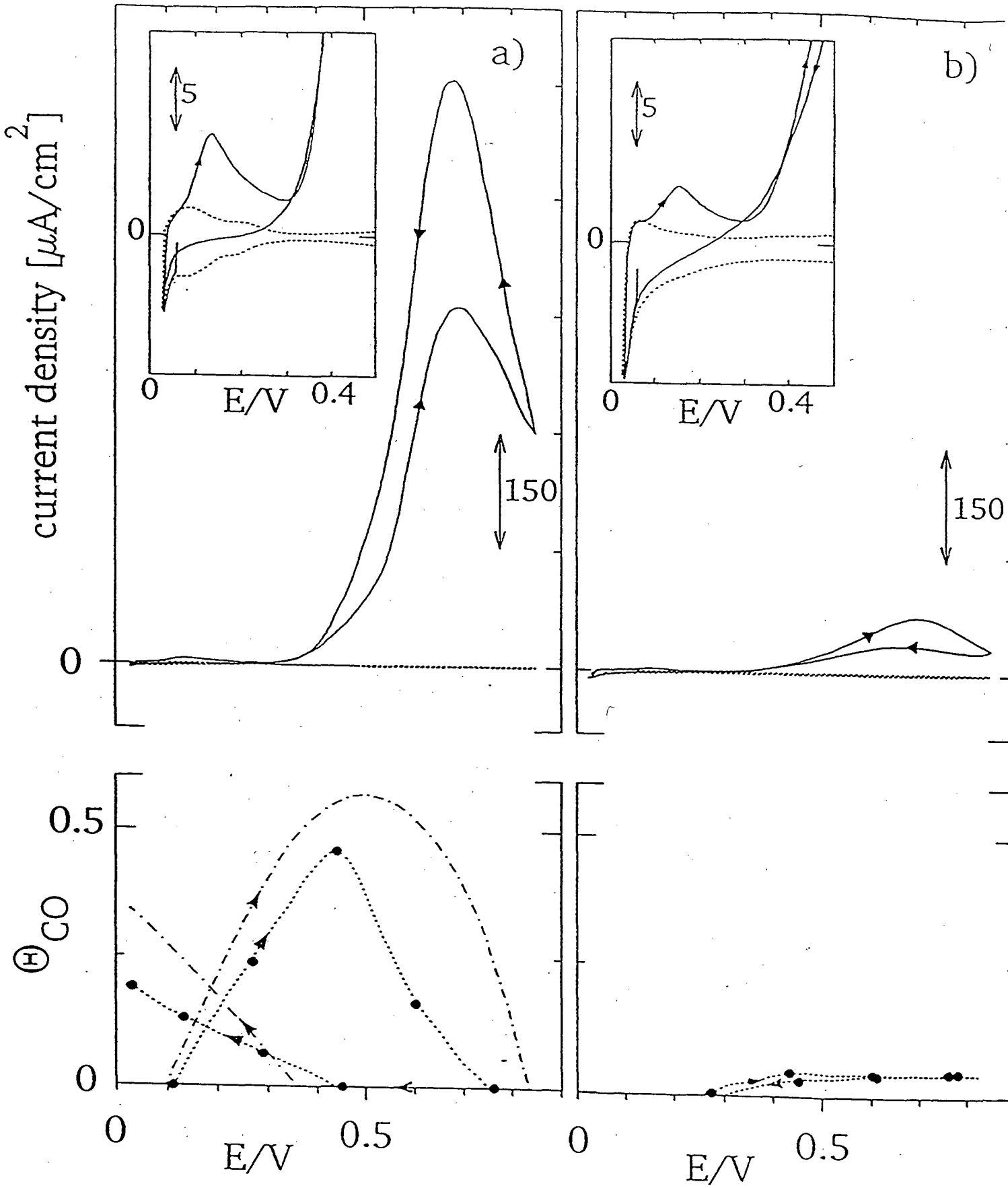

Fig. 12

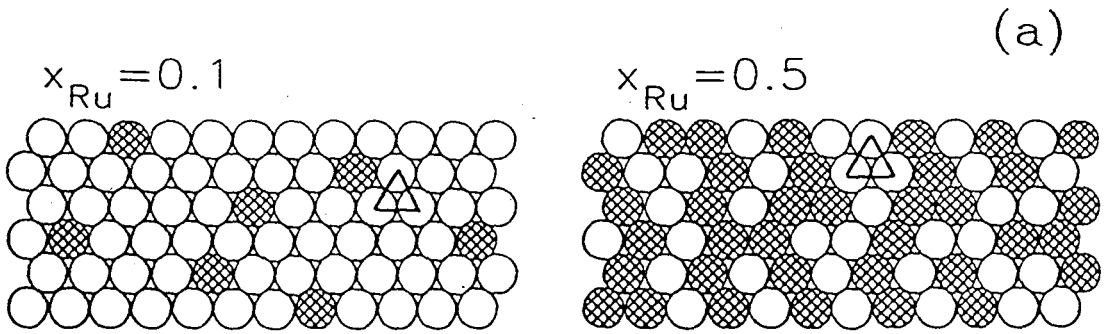
(a)
x_{Ru}=0.1
x_{Ru}=0.5

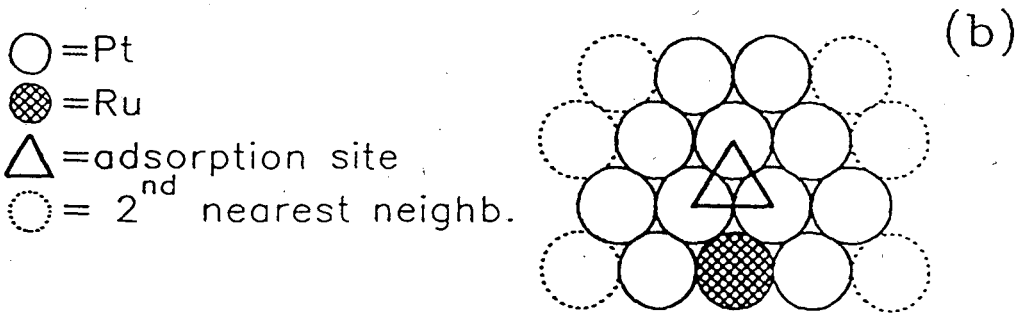
=Pt
=Ru
=adsorption site
= 2nd nearest neighb.
(b)

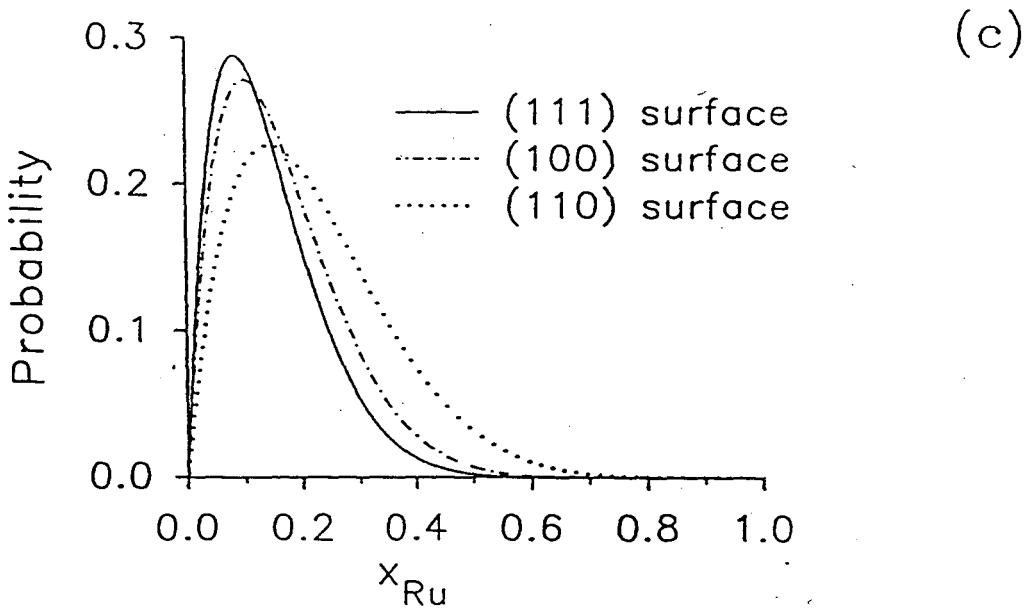
(c)
Probability
0.0
0.1
0.2
0.3
0.0
0.2
0.4
0.6
0.8
1.0
x_{Ru}
(111) surface
(100) surface
(110) surface

Fig. 13

Ernest Orlando Lawrence Berkeley National Laboratory
One Cyclotron Road | Berkeley, California 94720

Prepared for the U.S. Department of Energy under Contract No. DE-AC03-76SF00098